ELSEVIER

Contents lists available at ScienceDirect

## Journal of Hydrology

journal homepage: www.elsevier.com/locate/jhydrol



## Research papers



# Impacts of alternate wetting and drying and delayed flood rice irrigation on growing season evapotranspiration

Colby W. Reavis<sup>a,\*</sup>, Kosana Suvočarev<sup>a,c</sup>, Michele L. Reba<sup>b</sup>, Benjamin R.K. Runkle<sup>a</sup>

- a Department of Biological and Agricultural Engineering, University of Arkansas, Fayetteville, AR, United States
- b USDA ARS Delta Water Management Research Unit, Jonesboro, AR, United States
- <sup>c</sup> Department of Land, Air, and Water Resources, University of California-Davis, CA, United States

#### ARTICLE INFO

This manuscript was handled by Marco Borga, Editor-in-Chief, with the assistance of Edoardo Daly, Associate Editor

Keywords:
Evapotranspiration
Rice
Alternate wetting and drying
Penman Monteith
Eddy covariance

#### ABSTRACT

As rice production is water intensive, establishing an accurate field-scale water budget is paramount for sustainable use of local water resources. This study's goal was to quantify and characterize half-hourly and seasonal evapotranspiration (ET) in two commercial, zero-grade rice fields in the U.S. Mid-South over three growing seasons. During each growing season, irrigation regimes for the studied fields differed between alternate wetting and drying (AWD) and delayed flooding (DF). The 2015 growing season enabled a direct comparison of the effects of AWD and DF on ET, while during the 2016 and 2017 seasons both fields were simultaneously under AWD and DF, respectively. The DF method is the region's most common irrigation practice, and it prescribes a continuous flood to be maintained for the majority of the growing season after the plants have reached the 5-leaf growth stage (40-50 days after planting). In contrast, after holding this initial flooding for 3 weeks, AWD allows for field drying to promote the capture of seasonal rains to reduce irrigation water withdrawal and associated water pumping costs. In this study, ET was estimated using gap-filled eddy covariance observations and two variations of the Penman-Monteith equation. These methods determined growing season ET values between 560 mm and 636 mm. This study found that there were no significant differences in cumulative ET or yield when comparing AWD to DF practices. Furthermore, AWD elicited no change in ET during periods of drying when compared to DF. By this metric, AWD did not induce drought stress within the plants. We conclude that the main benefit of the AWD practice is to take advantage of seasonal rainfall to offset pumping costs and pressure on irrigation water requirements while maintaining yields comparable to conventional irrigation practices.

## 1. Introduction

Water resources are currently consumed at unsustainable rates within the Lower Mississippi River Basin, where a majority of rice is grown in the United States (Kresse et al., 2014; Reba et al., 2013). Due to this depletion, the region is increasing efforts to conserve water and quantify water use, particularly by agricultural irrigation for its sustainable future management (Reba et al., 2017). To promote sustainable water use in rice production, various methods and technologies are being applied, such as field levelling to zero–grade, which can reduce irrigation water use by up to 40% (Henry et al., 2016), and multiple inlet irrigation, which can reduce water use by up to 24% (Massey et al., 2014, 2017, 2018). Alternate wetting and drying (AWD) is a practice that can potentially reduce irrigation water use by up to 20% by

capturing rain during the growing season, offsetting pumping costs for the producer (Carrijo et al., 2017; Pan et al., 2017; Lampayan et al., 2015). Prior to the onset of the initial flood in both AWD and delayed flood (DF) practices, the rice germinates and establishes in non–flooded soils (Moldenhauer et al., 2013). The recommended AWD practice allows periodic paddy drying, which lasts approximately 5 days, to occur at least 3 weeks after the first flooding. The conventional DF practice maintains a constant flood once the first flood is established until the fields are drained for harvest. However, the level and timing of drying induced in AWD are management decisions based on irrigation infrastructure, precipitation forecasting, soil type, plant variety, growth stage, and water supply. While AWD conserves water, there are concerns regarding plant health, grain quality, and decreases in yield compared to conventional growing practices (Graham-Acquaah et al., 2019; Norton

E-mail address: creavis@uark.edu (C.W. Reavis).

<sup>\*</sup> Corresponding author at: Department of Biological & Agricultural Engineering, University of Arkansas, 228 Engineering Hall, 1 University of Arkansas, Fayetteville, AR 72701, United States.

et al., 2017; Sudhir-Yadav et al., 2012); therefore, the timing and duration of the dry periods needs careful management. AWD is also expanding in use because of its potential to reduce greenhouse gas emissions associated with rice production (Linquist et al., 2015a, 2015b, 2018; Runkle et al., 2019).

Fields managed with AWD have the potential to reduce evapotranspiration (ET) when compared to conventionally managed fields due to the decline of available water at the soil surface and alteration of land surface radiative properties, which may reduce the amount of open water or soil water evaporation (Norman et al., 1995; Liu et al., 2019a, 2019b). However, ET is typically dominated by the plant-mediated release of water (transpiration), especially during the later portion of the growing season when the rice canopy is fully developed (Wei et al., 2015, 2017). The water savings for AWD are primarily seen in the capturing of rain events during drying periods. Ideally, the amount of rainfall captured during these events should offset the amount of pumped water required to replace water lost through ET (Kima et al., 2015). In rice water budgets and irrigation schedulers, producers use ET to estimate the amount of water required to sustain crop production without incurring stress (Li and Cui, 1996; Smith, 1992). Understanding how ET changes throughout the growing season also provides an indication of canopy health (Moran et al., 1995). ET is tied to primary production of plant biomass as water release from the plant is regulated by stomatal control, which helps dictate assimilation of carbon dioxide within the plant during the daytime (Ikawa et al., 2018; Roel et al., 1999; Wang et al., 2020). Because AWD has the potential to conserve water resources and provide economic benefits to the producer (Nalley et al., 2015), uncertainty within the terms of the water balance (including ET) must be reduced through careful measurement.

In agricultural settings, ET is typically estimated using approaches such as the Hargreaves or Penman-Monteith equations, which rely on meteorological data and basic estimates of phenology (Allen et al., 1998; Hargreaves and Allen, 2003; Pereira et al, 2015). However, studies conducted in rice have indicated sizeable differences when comparing measured ET, using micrometeorological approaches such as the eddy covariance method, and ET estimated with variations of the Penman-Monteith equation (Ikawa et al., 2017; Wang et al., 2017). These approaches include the Penman-Monteith method for actual ET (PM-AET) and the Penman-Monteith method as outlined in FAO Document 56 (PM-FAO56) (Monteith, 1965; Penman, 1948; Allen et al., 1998). Methods such as the PM-AET are of interest as their improvement would provide a platform for relating associated changes in measured ET to physically derived relationships between ET and multiple meteorological and phenological variables contained within the PM-AET. Many studies have identified areas of improvement for different implementations of the Penman-Monteith equation by focusing on different components, including canopy conductance and variable crop coefficients (Lecina et al., 2003; Alberto et al., 2014; Yan et al., 2018).

A common application of conductance is the "big leaf" approach that treats conductance as a bulk value across all leaves in the canopy, where its parameterization can be completed using only observations of local meteorological variables, LAI, and ET observations. However, single

layer conductance models typically underperform in periods of sparse (LAI < 2) vegetation (Xu et al., 2018; Lafleur and Rouse, 1990). Duallayer conductance approaches that address canopy and soil as separate contributors to ET have been recommended to address the poor performance of the PM-AET under sparse vegetation, including rice (Shuttleworth and Wallace, 1985; Facchi et al., 2013). Studies utilizing both the dual-layer and single layer conductance frameworks in rice have shown comparable performance between each approach during the growing season (Gharsallah et al., 2013; Liu et al., 2020).

Here, we quantify ET rates from within two fields in the humid U.S. Mid-South and compare AWD and DF irrigation management practices. The primary aim of this study is to better characterize half-hourly and seasonal ET in this region and identify associated impacts of altering the conventional irrigation regime with respect to ET. For this aim, we test whether fields with AWD irrigation show reduced ET relative to the DF field due to the lack of a free water surface during drying events by quantifying ET using different methods across multiple growing seasons. We then examine how ET changes during drying events to observe the effects drying has on plant activity. We assume that during drying events, if the plants undergoing AWD remain unstressed, the differences in transpiration should be negligible. Because transpiration makes up a large portion of ET during the growing season, we hypothesize that canopies with similar transpiration rates will show little differences in ET once the canopy is established. The second aim is to evaluate the performance of two accepted estimation methods in comparison to eddy covariance observations within both DF and AWD fields across the 2015–17 growing seasons. Finally, we seek to compare crop coefficients derived from local estimates of reference ET and eddy covariance to the crop coefficients for rice recommended in the FAO 56 document.

#### 2. Materials and methods

#### 2.1. Site description

The study site is composed of two adjacent commercial fields (~24 ha each) located in eastern Arkansas, USA (34° 35′ 8.6″ N, 91° 45′ 05″ W). The fields have been used to grow rice in continuous rotation since 2004 and are zero–graded with no slope within the planted area of the field. For this study, the fields are identified as North Field (NF) and South Field (SF). The soil within the fields is primarily characterized as poorly drained Perry silty clay (USDA classification: very-fine, smectitic, thermic Chromic Epiaquerts), which represents 100% of NF and 93.2% of SF (Runkle et al., 2019; Soil Survey Staff, 2018). The remaining portion of SF soil (~2 ha) is a Herbert silt loam (fine-silty, mixed, superactive, mesic Udollic Epiaqualfs). The composition of the soil varied between NF and SF where NF had greater clay content (62% vs. 43%). The fields are connected in a series of five similarly-sized fields where irrigation water is delivered across each field, moving north to south, before arriving at the desired field.

The rice was drill seeded and the growers apply the first flood approximately 47 days after planting (DAP). Rice grown within the fields in each study year was a hybrid variety (Clearfield XL745, Rice-Tec, Inc., Alvin, TX, USA) and followed the typical growing season for

Table 1
Seasonal Irrigation and first flooding dates for North Field (NF) and South Field (SF) during the 2015–2017 growing seasons. Irrigation practices presented are delayed flood (DF) and alternate wetting and drying (AWD). First flooding is presented with the flooding date and days after planting (DAP).

Field	Year	Irrigation Treatment	Planting Date	First Flooding		Harvest Date
				Date	DAP	
NF	2015	DF	8-Apr	14-May	40	19-Aug
	2016	AWD	23-Apr	14-Jun	52	13-Sep
	2017	DF	10-Apr	17-May	37	26-Aug
SF	2015	AWD	8-Apr	15-May	41	19-Aug
	2016	AWD	23-Apr	16-Jun	54	13-Sep
	2017	DF	9-Apr	18-May	38	27-Aug

rice in Arkansas from early April to September. The 2015–2017 growing seasons for NF and SF ranged 133–143 days from planting to harvest (Runkle et al., 2019). Irrigation during the growing season relies primarily on surface water, which travels between fields by gravity flow through pipes and ditches. Irrigation routes are set up so that water must flow through each field as a series running north to south. The irrigation treatments were altered between the three growing seasons (Table 1). In 2016, seeding was delayed due to wet field conditions, and, thus, the first flood was established later in the summer compared to 2015 and 2017 (i.e., 14 Jun vs. 14–17 May).

Instrumentation consisted of eddy covariance and biometeorological sensors (Runkle et al., 2019) and was identically installed in both fields. These measurements contribute to the Ameriflux Management Project (NF:US-HRC and SF:US-HRA) and its subnetwork Delta-Flux for responding to questions on sustainable practices in agriculture (Runkle et al., 2017). Due to the homogeneous fetch requirements for the eddy covariance technique, the equipment was installed on the northern edge of each field at approximately half the distance of the northern border to capture the dominant southern winds during the growing season, and fluxes north of each field were discarded. Equipment was installed approximately 15 m from the north edge of each field after drill-seeding and removed immediately prior to harvest. Deployment during the growing season normally occurred within 4 days post-planting, and removal of equipment occurred 2 days prior to harvest. Fluxes collected at the towers using eddy covariance were screened to include only wind directions between 95 and 265° to ensure measurement footprints were limited to their respective fields. Gaps within the observed fluxes for all three years were empirically filled using an artificial neural networks approach (Knox et al., 2015, 2016). This method used the following explanatory variables: days since the start of the study period, leaf area index (LAI), plant height, friction velocity (u\*), air temperature (T), incoming solar radiation (Rg,in), vapor pressure deficit (VPD), water depth (WD), and fuzzy transformation sets representing seasonality and time of day (see Runkle et al., 2019 for more details). The turbulent energy flux models correlated with observations with  $R^2$  values >0.90.

#### 2.2. Measurement of fluxes, microclimate, and plant parameters

The eddy covariance (EC) system provided measurements of sensible heat (H) and latent heat (LE) flux through the net exchange of the scalars, temperature and H2O, respectively. The EC system included a 3D sonic anemometer (CSAT3, Campbell Scientific, Inc., Logan, UT, USA) and an open-path infrared CO<sub>2</sub>/H<sub>2</sub>O analyzer (LI-7500A, LI-COR, Inc., Lincoln, NE, USA). The EC system was mounted on a tripod, with the sensor height measuring 2.2 m above the surface of the rice field. Separation for the EC sensors was approximately 0.1 m and was accounted for with frequency correction factors and signal lagging, including flow distortion by transducer shadowing (Horst et al., 2015), described in Runkle et al. (2019) and Suvočarev et al. (2019). The EC components used a designated analyzer interface unit (LI-7550, LI-COR, Inc., Lincoln, NE, USA) with outputs recorded at 20 Hz and half-hourly fluxes calculated with EddyPro v. 6.2 software with the output including calculated flux, quality flags, and an analysis of the flux footprint throughout the growing season. Fluxes were screened based on multiple factors, including turbulence, dominant wind direction (southern winds), footprint size, and availability based on power failures. The flux footprint was used to only include periods where 90% of the data was measured within 350 m of the tower to remove the effects of measurement drift across adjacent fields (Runkle et al., 2019). The resulting data coverage for half-hourly sensible and latent heat fluxes after filtering ranged between 23% and 34% across the growing periods.

The four components of net radiation (RN) were measured (CNR4, Kipp & Zonen, Inc., Delft, NL) at a height of 2.0 m. Incoming and outgoing photosynthetically active radiation (PAR) was also measured using quantum sensors (LI–190SB, LI–COR, Inc., Lincoln, NE, USA) at 1.85 m. Air temperature (T) and relative humidity (RH) were measured

using a shielded probe (HMP155A, Vaisala, Helsinki, FI). In addition to the sonic anemometer, wind speed and direction were also measured using a 2-D anemometer mounted at 3.2 m (05103-5 propeller wind monitor, R.M. Young, Traverse City, MI, USA). Soil heat flux (G) measurements were collected using two soil heat flux plates (HFP01, Hukseflux, Delft, NL) placed at different depths in each year: 8 cm, 5 cm, and 4 cm below the soil surface for the 2015, 2016, and 2017 growing seasons, respectively. Soil heat flux plate measurements were corrected for the stored energy in both soil and water column, using soil surface temperature and water temperature thermistor measurements (CS-107 (BetaTherm 100K6A1IA), Campbell Scientific, Inc., Logan, UT, USA). Thermistors were placed directly at the soil surface, 2 cm above each soil heat flux plate, and on a flotation device to capture the temperature of the changing flood level. The energy balance closure (EBC), as reported in Runkle et al. (2019), was calculated using sensible and latent heat flux from the EC towers, RN, and storage-corrected G at the half-hourly time step. For the 2015-2017 growing seasons, the EBC for NF was 0.73, 0.75, and 0.69, respectively, and 0.89, 0.69, and 0.82 for SF, respectively.

Volumetric water content measurements were collected using soil moisture Time Domain Transmissometer probes (SDI-12, Acclima, Sydney, AU) at 8 cm and 15 cm for all fields during all growing seasons. Measurements of WD were collected continuously using a piezometric sensor (Series 46x, Keller USA Inc., Fort Mill, SC, USA), vented for automatic compensation for barometric pressure changes, installed 30 cm from the tower in a perforated tube reaching approximately 30 cm below the soil surface. Other field parameters including plant density and soil bulk density were collected manually at different times during the growing season (Runkle et al., 2019). Bulk density and soil temperature above the soil heat flux plate were used in conjunction with WD measurements to correct for changes in heat storage in the water and saturated soil matrix above the plate during flooded and dry conditions (Fuchs and Tanner, 1968; Runkle et al., 2019).

## 2.3. Leaf area index (LAI) and canopy height model

To characterize changing canopy conditions and provide necessary inputs for the Penman-Monteith approach and EC processing, canopy height measurements were collected throughout the growing season and averaged across 10-measurements during each field excursion (approx. twice monthly, but less frequently in 2016; see below). Because of high crop uniformity, canopy height measurements were taken only within 30 m of the EC station, and represented the height from the soil surface to the height of the canopy top at eye level, ignoring flag leaves. LAI was measured at similar intervals using a plant canopy analyzer (LAI-2200C, LI-COR, Inc., Lincoln, NE, USA), averaging three samples taken within 30 m of the EC tower, per measurement period. Typically, sampling for LAI did not begin until the canopy achieved a measurable level of growth, usually 50-60 DAP when the canopy height was approximately 0.5 m. We estimated LAI and canopy height throughout the growing season with a growing-degree-day (GDD) model (Yang et al., 1995). This approach uses GDD as the cumulative sum of the differences between the mean daily temperature (T<sub>mean,daily</sub>) and a base temperature (Tbase). In this setting, Tbase was set as 10  $^{\circ}\text{C}$  to represent the minimum temperature for growth and development in rice (Keisling et al., 1984).

LAI and canopy height data were collected through field measurements during the 2015–2017 growing seasons in both the NF and SF. LAI observations were complemented with MODIS Terra (AM) satellite LAI (MOD15A2H; Myneni et al., 2015) to remedy gaps in field measurements and improve model timing regarding canopy development. The MODIS data provided information about rice canopy dynamics, most notably the transition to a phase of rapid growth (approximately 45 DAP) as the rice canopy transitioned from the vegetative to reproductive stages. The 1–km MODIS pixel encompassed vegetation from both studied fields (Fig. 1). The area surrounding the experimental fields are also rice paddies with similar phenological development.



**Fig. 1.** MODIS pixel (1–km) in red used for both NF and SF fields also known as US–HRC and US–HRA, respectively, in the Ameriflux Management Project. Pixel taken from ORNL MODIS Web Interface (Myneni et al., 2015; ORNL, 2018); Background image from Google Earth (imagery date, 14 October 2015). Towers include eddy covariance equipment. (For interpretation of the references to colour in this figure legend, the reader is referred to the web version of this article.)

For the 2015 and 2017 growing seasons, field observations collected with the LAI-2200C (n = 8 and n = 13, respectively) were necessary to model LAI as a linear and quadratic function of GDD during the early and rapid growth stages, respectively. In contrast, only two field observations (n = 2) of LAI were collected during the 2016 growing season in the early growth period. To compensate for lack of data in 2016, in that year the MODI5AH2 LAI product was used to estimate LAI (Myneni et al., 2015). To correct for the MODIS LAI product's consistent under--estimation bias (up to 20%) determined in 2015 and 2017, the MODIS data points used to model LAI during the 2016 growing season were adjusted using a scaling factor. This factor was estimated using a regression slope between measured data points and the MODIS data at the same time period for each field across the 2015-2017 growing seasons. The scaling factors (slopes) for each field were then applied to their respective MODIS data to generate a sufficient (n > 5) set of LAI data that could be used to identify linear and quadratic growth periods with respect to GDD during the 2016 growing season. A similar approach was applied to canopy height, where field data were collected and modeled based on the period of the growing season. Canopy height measurements were collected during the 2015-2017 growing seasons for each field within the study (NF and SF). The same approach used to model LAI before and after the transition from vegetative to reproductive stages was applied to canopy height, where the growth patterns before and after this transition were considered to be linear and quadratic, respectively, in relation to GDD.

#### 2.4. Methods for modeling ET

The PM–AET is based on meteorological data and information about plant development. The combination Eq. (1) is based on the latent energy requirement for evaporating water and the deficit of vapor pressure necessary for removing water. It also accounts for the resistances for transpiring the water from plant tissue and transporting it away from the crop canopy. It was used to evaluate data collected in real time from both fields at the 30–min time step.

$$\lambda ET = \frac{\Delta (RN-G) + c_p \rho_a VPD/r_a}{\Delta + \gamma (1 + r_s/r_a)} \tag{1} \label{eq:energy}$$

where  $\lambda$  is the latent heat of vaporization (2.45 MJ kg $^{-1}$ ), ET is evapotranspiration (mm day $^{-1}$ ),  $c_p$  is specific heat of air (J kg $^{-1}$  °C $^{-1}$ ),  $\rho_a$  is mean air density (kg m $^{-3}$ ),  $r_s$  is bulk surface resistance (s m $^{-1}$ ),  $r_a$  is aerodynamic resistance (s m $^{-1}$ ) derived from wind speed, canopy height, and measurement height of wind speed (see Appendix A),  $\Delta$  is the slope of vapor pressure–temperature relationship (kPa $^{\circ}C^{-1}$ ), and  $\gamma$  is

the psychrometric constant (kPa  $^{\circ}$ C $^{-1}$ ) determined as  $6.65*10^{-3}$   $P_{atm}$  (Atm). The PM–AET can be used to estimate stomatal conductance using EC data through inversion and is also one of the few methods that can generate an ET estimate at the half–hourly time scale using only meteorological data.

The PM–FAO56 method (Eq. (2)) generates daily estimates of reference ET (ET $_{\rm o}$ , mm day $^{-1}$ ) from a reference crop, a short, well-watered grass, and the crop ET (mm day $^{-1}$ ) is calculated using dimensionless crop coefficients:

$$ET_{c} = ET_{0}*K_{c} = \frac{0.408\Delta(R_{n} - G) + \gamma \left(\frac{C_{n}}{T + 273}\right)(VPD)u_{2m}}{\Delta + \gamma(1 + C_{d}u_{2m})}*K_{c}$$
 (2)

where  $ET_c$  is crop evapotranspiration (mm day $^{-1}$ ),  $ET_0$  is reference evapotranspiration (mm day $^{-1}$ ), T is mean daily air temperature at 2.0 m height ( $^{\circ}C$ ),  $u_{2m}$  is wind speed at 2.0 m height (m s $^{-1}$ ),  $C_d$  and  $C_n$  are coefficients based on canopy development for a theoretical crop at 0.12 m in height, and  $K_c$  is the crop coefficient for converting  $ET_0$  to rice canopy ET.

Each rice development stage has a corresponding crop coefficient. According to tabulated FAO56 values the crop coefficients for rice grown in a humid environment with moderately high wind speed (>2 m  $\,$  $s^{-1}$ ) are equal to 1.05, 1.20, and 0.9 for the initial, mid-season, and late-season periods of the growing season, respectively. The lengths of time used to define the initial, developmental, mid-season, and late season stages of rice crop growth are 30, 30, 80, and 40 days, respectively. The tabulated rice crop coefficients given were also derived from the water-seeded rice practice, where rice was deposited directly into pre-flooded paddies, based on the identical recommended values (1.05) for coefficient  $K_{c,ini}$  and open water surfaces. For this method, several assumptions were made in relation to the reference evapotranspiration and G. Reference evapotranspiration requires measurements taken from a representative plot that adheres to FAO 56 standards so that all other assumptions inherent to the model hold for representativeness of the evaporative demand of the atmosphere. The local USDA weather station in Stuttgart, AR (~20 km to east of site surrounded by similar agricultural fields) provided measurements of T, RH, u<sub>3m</sub>, and R<sub>g,in</sub>. The wind speed measurements from the weather station were corrected to u<sub>2m</sub> using the logarithmic wind speed profile approach outlined in FAO56. Additional components of RN were estimated using "missing climate data methods" outlined in FAO 56 based on the location of the site as well as the day of year. Daily ground heat flux G is assumed by FAO 56 to average to zero at the daily time step. The crop coefficient was also adjusted using modeled canopy height and relative humidity as outlined in FAO 56, Chapter 6 to account for differences between the field site and the sites used to derive the recommended crop coefficients (Allen et al., 1998). Both the recommended and adjusted crop coefficients were compared to the observed crop coefficients at our field site.

## 2.5. Estimating and modeling canopy conductance

Canopy conductance,  $g_c$ , is a key term within the PM–AET model that reflects biological mediation of the exchange of gases between the rice canopy and the surrounding atmosphere. To estimate  $g_c$  within each experimental field site, the PM–AET model was inverted (Eq. (3)) to solve for  $g_c$  using observed (non–gap–filled) EC measurements of ET (ET $_{EC}$ ) for the evapotranspiration term:

$$g_{c} = \frac{\lambda E T_{EC} ^{*} \gamma ^{*} g_{a}}{\Delta (R_{n} - G) + c_{p} p_{a} (e_{s} - e_{a}) g_{a} - \lambda E T_{EC} (\Delta + \gamma)} \tag{3} \label{eq:3}$$

Values of estimated  $g_c$  were limited to periods with positive  $ET_{EC}$ . The estimated  $g_c$  in these half–hour intervals was used to parameterize a model (Eqs. (4)–(8)), which utilized both meteorological and biological inputs to predict estimates of  $g_c$  in a Jarvis–style approach (Jarvis, et al., 1976; Xu et al., 2017; Ershadi et al., 2015; Gardiol et al., 2003). Surface

conductance,  $g_s$ , was determined through  $g_s = g_c \, LAI_{active}^{-1}$  where  $LAI_{active}$ , determined with Eq. (8), represents the active fraction of LAI (m<sup>2</sup> m<sup>-2</sup>) available for transpiration.

$$g_{c} = g_{s,max} * f(R_{g,in}) * f(VPD) * f(T) * LAI_{active}$$
(4)

$$f(R_{g,in}) = 1 - e^{\left(\frac{-R_{g,in}}{a_1}\right)} \tag{5}$$

$$f(VPD) = 1 - a_2 * VPD \tag{6}$$

$$f(T) = 1 - a_3 * (25 - T)^2$$
(7)

$$LAI_{active} = \begin{cases} 1 & LAI < 1\\ LAI & 1 \le LAI < 2\\ 2 & 2 \le LAI < 4\\ 0.5LAI & 4 < LAI \end{cases}$$
 (8)

where  $a_1$ ,  $a_2$ ,  $a_3$  are fitted parameters and  $g_{s,max}$  is the maximum surface conductance. The LAI<sub>active</sub> scales from  $g_s$  to  $g_c$ , to incorporate the effects of canopy development and associated driving forces on surface conductance across the rice canopy (Collatz et al., 1991; Leuning et al., 1995). The use of LAI<sub>active</sub> follows the "big leaf" approach for modeling conductance across landscapes (Zhang et al., 2008; Li et al., 2016; Xu et al., 2017). To prevent uneven weighting of LAI and contributing plant transpiration, the LAI<sub>active</sub> parameter was assigned to have a value of unity during the early growing season when surface evaporation would be most pronounced in ET. Maximum surface conductance ( $g_{s,max}$ ) was determined as the maximum  $g_s$  observation in a 7–day moving window across the entire growing season. Negative and pseudo–infinite values ( $g_s > 10^4 \text{ mm s}^{-1}$ ) were removed as well as values when incoming  $R_{g,in}$  radiation was  $< 30 \text{ W m}^{-2}$ .

For calibration and validation of the model, we conducted a random selection of the data across all six site years for each step. The calibration dataset represented 70% of the total dataset while the model and parameters were validated using the remaining 30%. The parameters for the conductance model were optimized using nonlinear regression of measured and modeled ET, and assessed by the slope,  $R^2$ , and RMSE of the regression. The parameters were calculated using nonlinear least squares regression between measured ET and modeled ET while fitting  $g_{\rm C}$  with parameters  $a_1$ ,  $a_2$ , and  $a_3$ ; thus, any uncertainty in the biometeorological inputs (in addition to measured ET) was also transmitted to the conductance term. The conductance parameterization only utilized data taken from 40 DAP and during the daytime period (8 AM to 6 PM, local time) to ensure that conductance terms were not estimated with influence from periods when the rice canopy was less likely to impact ET.

#### 2.6. Comparison and analysis of ET observations

To better understand impacts related to differences in irrigation treatment, we directly compared simultaneous ET observations (non--gap-filled) to other biometeorological factors. The variables tested included meteorological drivers in the Penman-Monteith equation, such as available energy and VPD, and variables tied to the soil conditions in each field, including volumetric water content (VWC) and WD. Modeled canopy height and LAI were included in this analysis to account for canopy differences. Ratios of H to RN were analyzed over the growing season to better understand how shifts in ET and canopy development affect the partitioning of available energy within the field energy balance. Cumulative estimates of ET were compared across growing seasons and irrigation treatments. The number of days missed due to the instrument deployment and pre-harvest removal averaged 6, 5, and 2 days across both fields for the 2015, 2016, and 2017 growing seasons, respectively. The estimates of cumulative ET were also normalized by DAP to calculate a seasonal ET rate absent of bias incurred by differences

in growing season length.

The 2015 growing season was the only growing season where the effects of drying could be compared using simultaneous observations between both fields throughout the entire growing season. In 2016 and 2017, both fields were kept under the same irrigation management, making it impossible to directly compare simultaneous ET observations during drying events occurring in a single field. Instead, comparisons for the 2016 and 2017 growing season provided an opportunity to observe the effects of drying by comparing periods where both fields were either wet or dry to determine the relative impacts of drying events during each month of the growing season. To assess the impacts of drying events on ET, analysis of covariance (ANCOVA) was used to determine if ET was significantly different between fields when one was wet and the other was dry using WD measured in both fields. The comparison was conducted on a monthly basis where "Wet" (WDDF > 0 & WDAWD > 0) and "Dry" (WDDF > 0 & WDAWD < 0) categories served as the groupings for ET, where the subscripts indicate the respective field irrigation treatment. To remain consistent with other comparisons between fields. this analysis was limited to measurements taken during the daytime (8 AM-6 PM, local time). For the purposes of this paper, we define a drying event as any period after initial flooding where WD in a field falls below the soil surface for at least 24 h. The analysis was also limited to AWD drying periods, meaning any data prior to initial flooding and after the beginning of final drainage was not included.

Comparisons between the modeled and observed ET were used to evaluate model performance using residuals analysis. Residuals from regressions between modeled and observed ET were compared to both meteorological and phenological variables within the respective fields to identify periods of higher and lower model performance. The approach would also determine what input variables are critical in determining ET in the U.S. Mid-South production setting as well as identifying variables that could be associated with differences between observed and modeled ET. Moreover, comparing performance across both PM methods allows a test of which methods are better suited for estimating ET and understanding dynamics of ET with respect to the local biometeorology. For the PM-FAO56 method, comparisons between modeled and observed values were limited to days where <40% of the original EC data between 8 AM and 6 PM were missing before gap filling using the ANN procedure. This measure was taken to limit the impact of completely gap-filled days while preventing uneven weighting within the non-gap-filled data set due to quality control based on turbulence and instrumentation

#### 3. Results

## 3.1. Meteorological observations

Across all growing seasons, the NF and SF sites maintained a mean daily temperature of 24.5 °C with values ranging between 10 °C (early April) and 36 °C (mid-July). Mean daily relative humidity was 80% with values ranging 22-100% during the early growing season (April and May) and 40-100% during the mid-late growing season (June-August) after the flood was applied. The mean daily VPD ranged between 0.5 and 1.7 kPa with maximum values exceeding 2.5 kPa during the daytime period (8 AM-6 PM, local time) with peak values typically occurring between 4 PM and 6 PM. Wind speed averaged 2.06 m s<sup>-1</sup> with maximum speeds exceeding 10 m s<sup>-1</sup>. Mean incoming solar radiation was 248 W m<sup>-2</sup> across all growing seasons with maximum measured values  $>\!1000~\text{W}~\text{m}^{-2}$  occurring between mid-June and early July, and maximum values typically occurred between 12 h and 14 h. Comparisons to the 30-year (1981–2010) average showed that monthly mean temperatures were always within 2 °C of normal (Runkle et al., 2019). Comparison of precipitation during the growing season months of April to August showed that all three growing seasons were wetter than the 30-year normal of 492 mm, with 505 mm in 2015, 627 mm in 2016, and 868 mm in 2017. For all three measurement seasons, 40-60% of the growing season precipitation occurred in April and May.

#### 3.2. Canopy height and LAI

By comparing MODIS data to collected LAI data, we were able to determine a shift from slow to rapid canopy growth, after emergence and the initial vegetative growth stages (Fig. 2). Due to different planting dates, this transition date varied among growing seasons, occurring between 40 and 50 DAP. Maximum LAI was achieved in the SF at 103, 89, and 99 DAP and 103, 89, and 94 DAP in the NF during the 2015–2017 growing seasons, respectively. Maximum LAI for the three respective growing seasons was 5.4, 6.5, and 5.6 for the SF and 4.5, 5.5, and 4.5 for the NF, respectively. Relative to other years, MODIS data for 2016 indicated a more rapid early growth and higher peak in LAI; while we do not have LAI-2200C measurements in this year, the canopy height measurements also show higher values.

For the 2015–2017 growing seasons, maximum canopy height was reached between 111 and 124 DAP for SF and between 109 and 130 days for NF (Fig. 3). Maximum canopy height for NF and SF ranged between 0.95 and 1.32 m and 0.93–1.24 m, respectively. Similar to observed LAI, the 2016 growing season had a taller canopy during the latter portion of the growing season when the canopy was fully developed. The timing of peak canopy height varied as well, occurring between 105 and 118 DAP across NF and SF, respectively. Based on our estimates of phenological development, both peak LAI and peak canopy height occurred near the end of the R4 reproductive growth stage and the beginning of grain filling.

#### 3.3. Growing season ET estimates and dynamics in 2015-2017

The observed and gap—filled growing season ET ranged from 560 to 636 mm across the three growing seasons in both fields (Table 2). The 2015 growing season showed the lowest cumulative ET across both fields. From planting to harvest, the lengths of the growing season were comparable between the fields (i.e., from 0 to 2 days difference). WD varied throughout each growing season, especially in the 2015 and 2016 growing seasons where AWD was applied to at least one field (Fig. 4).

For the 2015 and 2016 growing seasons, drying events lasted between 2 and 7 days when irrigation was interrupted, and the flood water

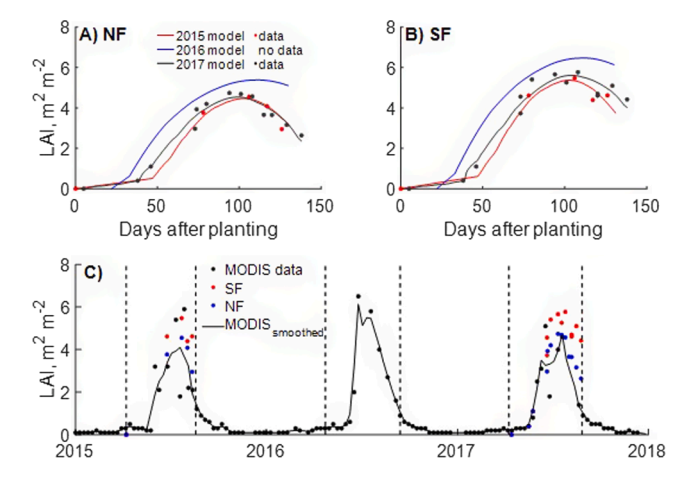


**Fig. 2.** Comparison between measured, GDD–modeled, and remote sensing LAI throughout the 2015–2017 growing seasons at: (A) the North Field (NF) and (B) South Field (SF), including the model in 2016 where LAI was directly scaled from MODIS without using direct measurements. Points displayed represent field observations made by the LAI-2200C; (C) smoothed (n = 5) and 8–day unscaled MODIS LAI time series from 2015 through 2017 with measured LAI points from the LAI-2200C for comparison, where black points represent MODIS data points, and dashed lines mark the planting and harvest dates for each year. The standard deviation of individual points ranged between 0.24 and 0.73 m $^2$  m $^{-2}$  throughout the growing season.

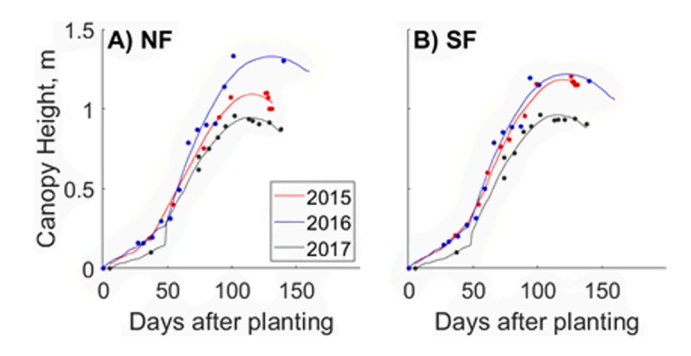


**Fig. 3.** Comparison between measured and GDD–modeled daily canopy height for the 2015, 2016, and 2017 growing seasons for NF (a) and SF (b) using DAP for inter-year comparison. Solid lines are the GDD–derived modeled values, while the dots represent measured values.

was evaporated. The minimum WD during drying events ranged between 2 and 30 cm below the soil surface prior to re–flooding. The soil moisture sensors at 15 cm below the soil surface indicated up to a 33 percentage-point reduction (saturation to minimum VWC) in VWC during drying events. Volumetric water content measured during drying events in both fields during the 2015 and 2016 growing seasons did not fall below 20% compared to 58% soil moisture at saturation during inundation. The producers reestablished the flood based on presumed soil dryness and observed decline in the water depth, corresponding to a WD of between 25 and 30 cm below the soil surface measured at the EC tower.

Using the gap-filled eddy covariance observations, cumulative growing season ET was calculated for NF and SF for the 2015-2017 growing seasons (Table 2). There were no clear relationships between irrigation treatment and estimated daily ET rate, as AWD and DF fields produced overlapping ranges of estimated daily ET rates during the 2015–2017 growing seasons. There were also no distinguishing patterns when only looking at the daytime ET, therefore irrigation regime did not seem to play a major factor in determining growing season ET for NF and SF during the 2015-2017 growing seasons. Fields under AWD management averaged 609 mm while fields under DF management averaged 595 mm, which were not significantly different. In relation to cumulative seasonal precipitation across both fields during the growing season, ET exceeded growing season precipitation in 2015 and 2016 by as much as 20% while only accounting for up to 78% of growing season precipitation in 2017, when precipitation events were unusually frequent. However, the precipitation event dynamics did not match the crop water requirements and some irrigation applications were necessary to regulate the flood levels.

Next, we compared treatments at the half hourly time step to test the effects of AWD and DF on ET across both fields for the 2015–2017 growing seasons using ANN gap–filled half–hourly ET. The period of observation was limited to daytime values between 8 AM and 6 PM to prevent uneven weighting from nighttime periods. This comparison also confirms, despite having different irrigation regimes, there were no significant differences in ET during the 2015 growing season (Fig. 5). Comparisons of ET measured in 2016 and 2017, when both fields were in the same irrigation treatment, showed similar results as well. In addition, these results did not change significantly when only observed values (i.e., not gap–filled data) were used for comparison.

NF showed consistently similar LE compared to SF. In 2016, NF had slightly higher ET based on a linear regression slope of 0.96. The slopes of each regression were significant with the slope standard error across all three comparisons, never exceeding 0.00042. For comparisons between NF and SF across 2015–2017, RMSE ranged between 1.02 and 1.68 mm day<sup>-1</sup> with a majority of the divergence occurring earlier in the growing season. The divergence in ET during the early growing season, when the soil water or water evaporation components dominate the ET

**Table 2**Estimated growing season (GS) ET from gap-filled EC observations, seasonal Daily ET rate, and Daytime ET for NF and SF during the 2015–2017 growing seasons.

Field	Year	Irrigation Treatment	Growing Season ET [mm]	Growing Season Length [days]	Avg. Daily ET Rate [mm day <sup>-1</sup> ]	Growing Season Precipitation [mm]
NF	2015	DF	$551 \pm 7.1$	133	4.14	500
	2016	AWD	$601\pm10.5$	143	4.20	556
	2017	DF	$628 \pm 6.9$	138	4.55	795
SF	2015	AWD	$598 \pm 14.0$	134	4.46	500
	2016	AWD	$604 \pm 9.7$	143	4.22	556
	2017	DF	$579\pm13.4$	140	4.13	795

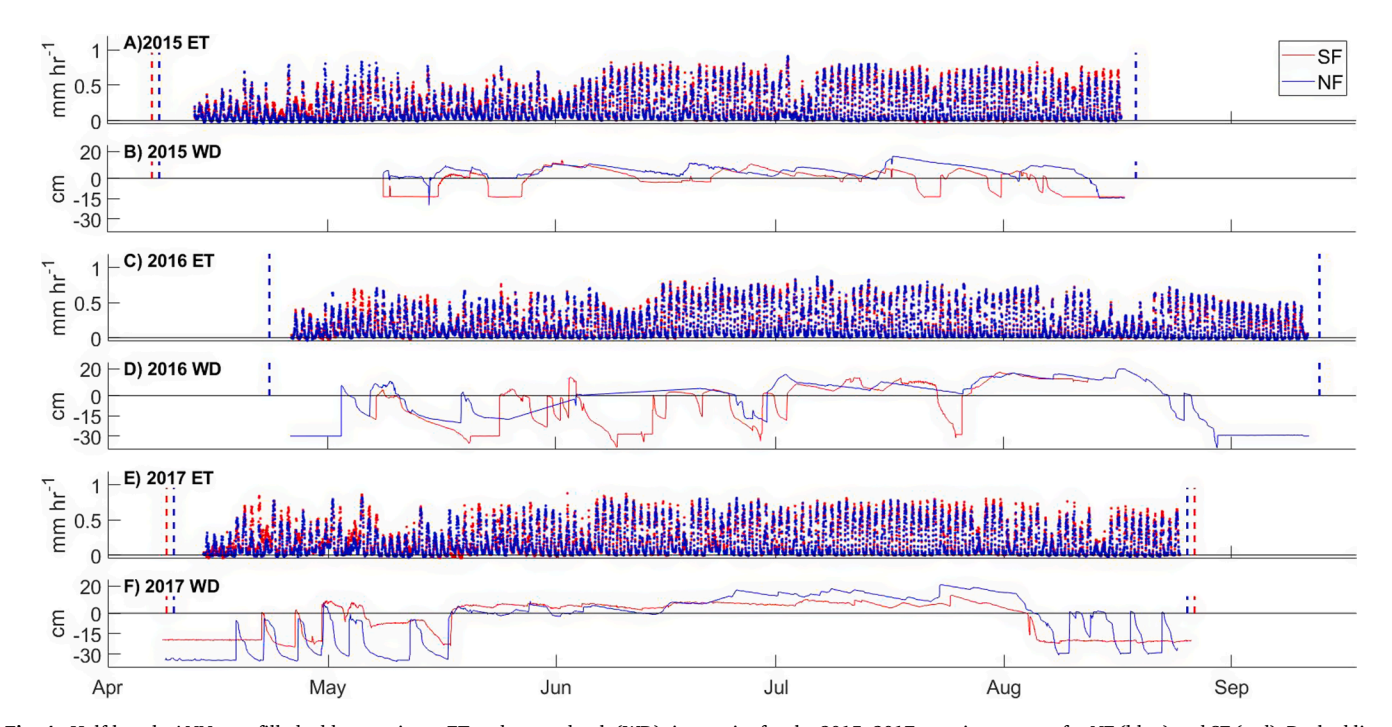


**Fig. 4.** Half-hourly ANN gap-filled eddy covariance ET and water depth (WD) time series for the 2015–2017 growing seasons for NF (blue) and SF (red). Dashed lines mark planting and harvest for NF (blue) and SF (red) (NOTE: The planting date was the same in 2016 for both fields, and harvest dates were the same in 2015 and 2016 for both fields). (For interpretation of the references to colour in this figure legend, the reader is referred to the web version of this article.)

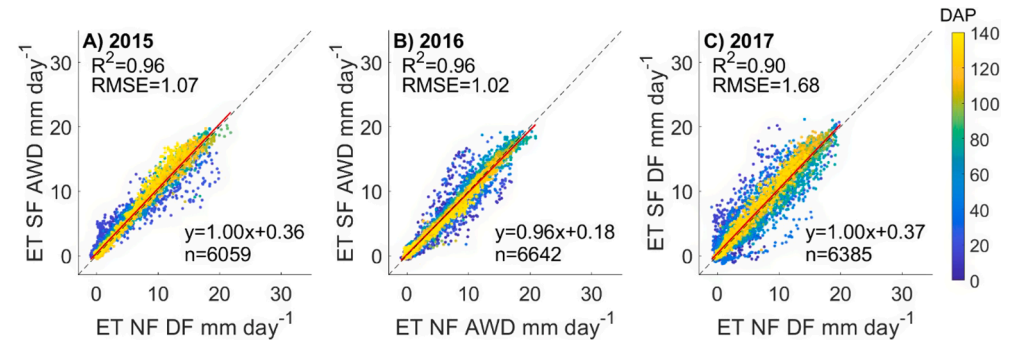


Fig. 5. Comparison of half-hourly ANN gap—filled eddy covariance evapotranspiration (ET) between the South Field (SF) and North Field (NF) during the 2015–2017 growing seasons, where the irrigation treatments are indicated (Alternate wetting and drying, AWD; Delayed Flood, DF). Points are colored by days after planting (DAP) (Note: In 2017, SF was planted a day earlier than NF, but the coloring represents DAP for SF only).

process, was due to different planting and flooding schedules for each field. Events where one field was flooded first before the other indicate higher ET, and these events are especially common during the early growing season (e.g., the cluster of points in Fig. 5c extending to 16 mm day<sup>-1</sup> in NF and 8 mm day<sup>-1</sup> in SF). Typically, once the canopy was established, the fields converged in terms of ET and continued to do so through closure until they were drained for harvest. Based on our observations, development and closure of the rice canopy clearly reduced the impact of factors of change in ET between both fields, including

factors related to their respective irrigation treatments such as water level or soil moisture.

There were no significant differences in the measured RN between NF and SF across all three growing seasons. The majority of ET was driven by RN with the ratio of LE to RN throughout the growing seasons ranging between 0.71 and 0.85. For individual months, particularly July and August, LE measured between 55 and 75% of RN while in early periods of the growing season (April and May), LE ranged between 24 and 51% of RN. The ratio of H to RN consistently decreased from the

beginning of the growing season until pre–harvest draining, when the ratio of H to RN increased in most cases. Given that the variation of RN was minimal during the growing season, this decrease in the ratio of H to RN was most likely due to the increase in LE associated with flooding, canopy development, and greater amounts of transpiration.

#### 3.4. Effects of AWD on ET in eddy covariance observations

In order to test the effect of AWD on ET variation due to changing flood water availability for evaporation, parts of the 2015 growing season with drying events in SF and inundation in NF field were used to compare the simultaneous ET values. The length of drying events was consistently around 1 week. Our results indicate that prior to canopy development and closure, specifically in May 2015 when dry and wet conditions were being compared directly, there is a significant difference (p < 0.05) in measured ET (Table 3). While there were significant differences in ET, these drying events were not carried out as part of an AWD treatment as the first permanent flood had yet to be established.

In May 2015, the slope of 0.91 indicates that drying period ET was 9% greater in the inundated NF compared to the non-flooded conditions in SF. During this period, both fields did not have a developed canopy, and only one drying event had occurred. While we do not consider the significant differences in ET to be a direct result of the AWD treatment in NF, analysis between the residuals taken from the initial field-to-field regression and the declining WD in SF indicated that the drying significantly explained only up to 5% of ET residual variance. All other months during the 2015 growing season indicated no significant difference in observed ET across all hydrological conditions, and declining WD in the drying field was unable to explain any significant differences observed in ET between NF and SF. We suspect that differences occurring early in the growing season are substantially influenced by precipitation as well in altering the plant canopy response with respect to ET. Additionally, in this farm setting, precipitation can be managed in a way that water is actively drained between fields along a designated

**Table 3**ANCOVA analysis of NF vs. SF ET observations across different hydrological scenarios throughout the growing season. Values are slopes between a number, n, of simultaneous 30–min ET estimates in each field. "Wet Condition" refers to periods when both fields are wet, defined as having a water level above the soil surface in both fields. "Drying Condition" refers to periods where drying occurred in one or both fields with drying considered as a decline in the WD below the soil surface for given field(s).

Year	Month	Number of AWD drying events		Tota dura of dr even days	tion ying ts,	Wet Condition slope (n)	Drying Condition slope (n)	
		NF	SF	NF	SF			
2015	May	0	1	0	5	1.05 (110)	0.91 (34)*	
	June	0	2	0	10	1.01 (124)	1.06 (152)	
	July	0	2	0	8	0.96 (286)	0.96 (22)	
	August	0	1	0	1	0.91 (18)		
2016	May	0	0	0	0	0.75 (18)		
	June	1	3	4	7	0.85 (63)	$0.99(31)^{\dagger}$	
	July	0	1	0	3	0.93 (262)		
	August	0	0	0	0	0.93 (161)		
2017	May	1	0	2	0	0.77 (36)		
	June	2	0	4	0	0.99 (170)		
	July	0	0	0	0	1.01 (293)		
	August	0	0	0	0	1.04 (15)		

<sup>\*</sup> Denotes significantly different "Drying Condition" slope compared to "Wet Condition" slope.

flow path (NF to SF) to prevent unsuitable growth conditions for the crop during early growth stages.

The canopy development stages explain the convergence of ET between the two fields and the inability of changes in WD to explain significant differences in ET during the latter portion of the growing season. Because both canopies were similar in structure and showed no decreases in yield associated with drying events in 2015, we can conclude that plant—mediated transpiration was likely similar in both fields. As the canopy continued to develop, the contributing portion of transpiration to ET increased, resulting in similar ET rates across both fields when the canopy was fully closed and developed. Canopy cover also likely exercised control over open water surface evaporation through shading, meaning the contributing portion of evaporation to ET likely decreased as well. This would result in insensitivity to ET and differences between fields with respect to water level.

In 2016 and 2017, there were no periods where only one field was dry since both fields were treated in AWD and DF, respectively. The columns in Table 3 for these years are therefore during periods when both are dry. During the 2016, slopes from the "All Wet" case did not significantly differ from slopes in the "All Dry" case across the growing season. Under both conditions, NF appeared to always have greater ET compared to SF despite both fields undergoing the same treatment. Measured ET between both fields seemed to agree more during dry periods, but these slopes were not significantly different from their wet counterpart during each individual month. In 2017, when both fields were managed with DF throughout the entire growing season, the comparison indicated no significant differences in slopes from the comparison between wet and dry periods. Flooded conditions made it impossible to perform dry period analysis in June and July of 2017 as well. Based on the observations in 2016-2017, we can infer wetting and drying did not play a significant role in influencing differences in ET across both fields, meaning the field effect based on changing WD does not play a consistent, significant role in our ET comparisons. This finding supports our observation of similar ET between fields regardless of WD management across all growing seasons. The change in slope between NF and SF ET rates also indicated that the fields continued to converge on similar ET as the canopy developed during the growing season as the slope drew nearer to a value of 1 with each successive month. Given that both fields were treated using the same irrigation method in 2016 and 2017, this similarity was expected and supports the concept of decreasing impacts of changing WD and associated soil water evaporation throughout the growing season as canopy transpiration dominates

#### 3.5. Modeling canopy conductance for the 2015–2017 growing seasons.

Canopy conductance estimated using eddy covariance measurements for LE and the inverted Penman–Monteith equation was estimated using the full 2015–2017 dataset (including both NF and SF). Maximum applied surface conductance from the 7–day moving window ranged between 8 and 70 mm s $^{-1}$  across both fields for the 2015–2017 growing seasons with peak values occurring during periods characterized by increased canopy height and LAI. Parameterization was performed for individual site seasons and across all six site-years combined. The parameters and standard error were estimated for each growing season as well as the combined period of all growing seasons (Table 4).

#### 3.6. Modeling ET for the 2015-2017 growing seasons using PM-AET

After parameterization with 70% of the data during calibration with data from across all six field–seasons, the calibrated model performed well against the remaining data as a validation set. The parameterized PM equation estimated half–hourly ET with high correlation ( $R^2 = 0.84$ ;  $m = 1 \pm 0.0015$  mm day $^{-1}$ ; RMSE = 2.12 mm day $^{-1}$ ) during daytime periods of the growing season across all six site–years. Within each individual growing season, model performance was varied across each

 $<sup>^\</sup>dagger$  Marks comparisons of drying condition where both fields were dry (i.e., not 2015).

<sup>&</sup>lt;sup>1</sup> Total duration of drying event does not include period prior to first flooding or drainage period in late growing season, rounded to the nearest day based on half–hourly WD data.

**Table 4** Fitted parameters for the individual and combined growing seasons across NF and SF for 2015–2017. Standard error estimates in parentheses were derived from the MSE for each parameter associated with the regression; RMSE is presented in terms of the LE flux (where 28 W m $^{-2}$  is approx. equivalent to 1 mm ET).

Field	Year	a <sub>1</sub> [W m <sup>-2</sup> ]	a <sub>2</sub> [kPa <sup>-1</sup> ]	a <sub>3</sub> [°C <sup>−2</sup> ]	Mean $g_s$ , $max$ [mm $s^{-1}$ ]	RMSE [W m <sup>-2</sup> ]
NF	2015	2445 (85)	0.14 (0.02)	0.005 (0.0003)	30	23.50
	2016	2522 (189)	0.04 (0.06)	0.007 (0.0004)	24	34.48
	2017	1367	0.26 (0.02)	0.005 (0.0008)	22	32.11
SF	2015	1542 (63)	0.26 (0.02)	0.006 (0.0005)	32	30.16
	2016	2169 (130)	0.33	0.000 (0.0012)	20	40.26
	2017	826 (85)	0.31 (0.04)	0.006 (0.0009)	19	27.77
NF + SF	2015–2017	1659 (30)	0.31 (0.00)	0.003 (0.0003)	28	34.88

irrigation comparison scenario, but was still able to explain similar amounts of variance (Fig. 6).

Analysis of model performance across the growing season indicated that the largest portion of variance between model and observation was during the early portion of the growing season (<40 DAP) when the active fraction of LAI was the lowest. General performance across all three growing seasons was inconsistent as the model both overestimates ET by 2% in 2015 and 2016 and underestimates ET by 12% in 2017. During the 2017 growing season, there was greater precipitation than 2015 and 2016, which could explain the model's inability to accurately reflect changes in canopy ET in response to rain events and an elevated moisture status. A two–sample t–test indicated that mean  $g_{s,max}$  estimated across 2017 was significantly (p < 0.05) lower than mean  $g_{s,max}$  in 2015 and 2016 by as much as 60%.

## 3.7. Modeling ET for the 2015–2017 growing seasons using PM-FAO56

The PM–FAO56 method was applied to the 2015–2017 growing season measurements at the daily time scale and compared to daily ET measured using EC. Because we did not observe noticeable differences in ET between NF and SF for all three growing seasons (the average daily difference was only 0.027 mm), an average ET representing both fields was used when comparing to the FAO56 estimates at the daily time step. Estimates from the PM–FAO56 approach were consistently higher than EC estimates with cumulative seasonal ET amounts at 607, 709, and 660 mm for the 2015–2017 growing seasons, respectively. These values were 8, 105, and 81 mm greater than the seasonal ET as directly measured by

the EC. Adjusted estimates of ET from the FAO56 method for the 2015–2017 growing seasons were 611, 698, and 651 mm, which are 13, 94, and 72 mm higher from the observed seasonal values, respectively. The estimated crop coefficient curve was shown to vary greatly throughout the growing season when compared to the FAO56 recommended values, including cases where the coefficient was adjusted for nonstandard conditions (Fig. 7).

The agreement between estimated and recommended K<sub>c</sub> values was poor throughout the growing season. When comparing values of K<sub>c</sub> derived from gap-filled EC data to recommended values, daily values could vary as much as 80% higher or lower than the recommended values. Compared to data points from days containing less gap filling, variance is reduced by 40% in estimated K<sub>c</sub> across the growing season, but individual K<sub>c</sub> values are still underestimated up to 79% and overestimated up to 80% across both the recommended and adjusted K<sub>c</sub> values. Using only the non-gap-filled EC derived K<sub>c</sub> (red points in Fig. 7) across 2015–2017, we estimate the K  $_{c,~ini},$  K  $_{c,mid},$  and K  $_{c,end}$  to be 0.94  $\pm$  $0.03, 1.16 \pm 0.02$ , and  $0.95 \pm 0.11$ , respectively. Variability between the recommended and observed crop coefficients was noticeable in the early growing season due to the difference in irrigation practices between the FAO recommendation and our field site as mentioned in the methods, but values were within an acceptable margin of error for the mid and late growing seasons. When comparing ET rates between the PM-FAO56 method and the EC towers using data, we excluded data points from the initial 60 days to remove the variance introduced from K<sub>c. ini.</sub> We also limited observation to only include periods where >60% of the measured daytime (8 AM to 6 PM, local time) ET was present to reduce the amount of uncertainty introduced by ANN gap-filling (Fig. 8).

Our results indicated no clear seasonal pattern to increased performance of the PM-FAO56 method when considering only the mid and late growing season. Across all growing seasons, we observed a consisted overestimation of ET during the late season period (DAP > 115) in 2015 and 2016, but mid-season performance varied from year to year. The adjusted crop coefficients (not shown) provided no improvement when compared to the same EC observations. Similar to the PM-AET approach, we suspect that increased precipitation and regional differences in growth conditions between our site and the reference site could have resulted in an irregular canopy response and altered ET from both fields during the growing season. We observed the best performance of the PM-FAO56 method when both fields were under AWD treatment and the amount of precipitation was noticeably less than in 2017 (Table 2).

#### 4. Discussion

#### 4.1. Comparing ET across irrigation regimes

Mean growing season ET was estimated to be between 4.14 and 4.55 mm  $day^{-1}$  for DF and between 4.20 and 4.46 mm  $day^{-1}$  for AWD using gap–filled eddy covariance estimates. Thus, this is additional evidence

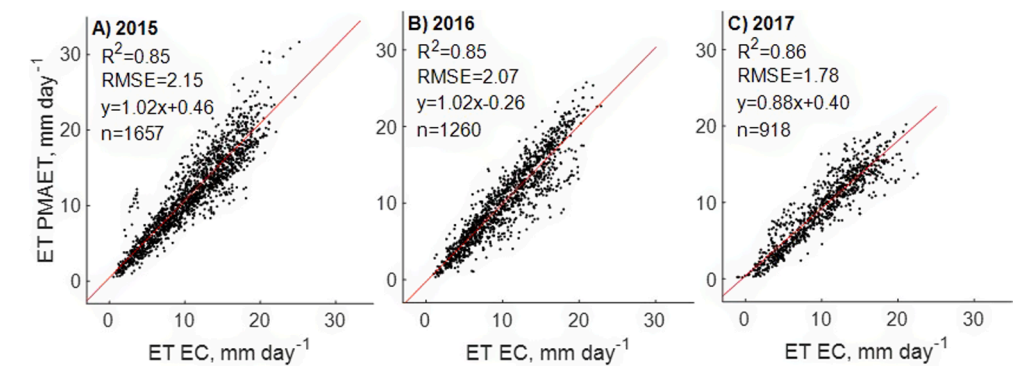


Fig. 6. Comparison of half-hourly PM model to non-gap-filled EC observations during the daytime period (8 AM to 6 PM, local time) across the 2015–2017 growing seasons and observations from both fields are plotted together.

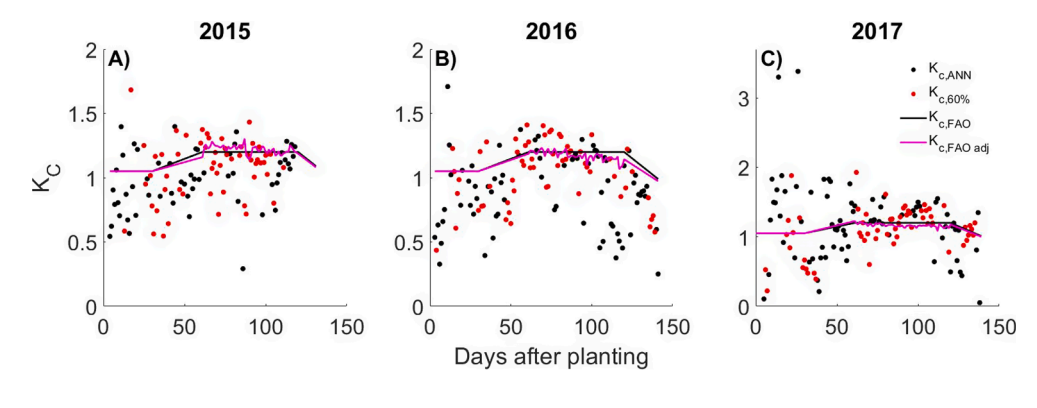


Fig. 7. Comparison of FAO56 recommended and adjusted crop coefficient (black and pink lines, respectively) and estimated crop coefficient ( $K_c$ ) using eddy covariance ET (black data points) for SF and NF during the 2015–2017 growing seasons (note change of scale for 2017). Red data points represent  $K_c$  values where >60% of the daytime (8 AM to 6 PM, local time) non–gap–filled EC ET data was available to help interpret the impacts of using only gap–filled data (Note y-axis scale change on C). (For interpretation of the references to colour in this figure legend, the reader is referred to the web version of this article.)

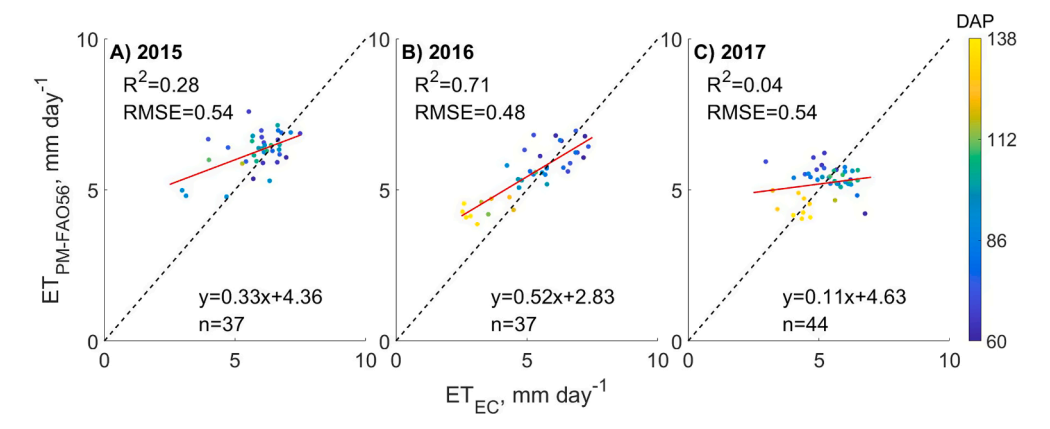


Fig. 8. Comparison of PM-FAO56 to EC-derived, gap-filled daily ET during the mid to late growing season across the 2015–2017 growing seasons. Points are colored by DAP.

**Table 5**Cumulative ET estimates and estimated daily ET rate during the growing season for different studies estimating ET in rice agriculture; EC is eddy covariance, PM is Penman–Monteith AET, PM–FAO56 is PM as defined in FAO56).

Seasonal ET (mm)	Growing Season Length (Days)	Equivalent Rate (mm day <sup>-1</sup> )	Location	Transplanted	Method	Study
813	122	6.66	CA–Water Seeded	No	Energy balance	Linquist et al., 2015a,
889	113	7.87		No	residual	2015b
856	115	7.44		No		
873	134	6.51	CA-Dry Seeded	No		
865	112	7.72		No		
875	116	7.54		No		
570	116	5.76	Namibia	Yes	Penman Monteith	Kotani et al., 2017
548	100	5.48	Hyderabad, India	Yes	Pan evaporation	Mote et al., 2018
499	117	4.25	IRRI	No	EC, PM	Alberto et al., 2014
562	132	4.26	Brazil	No	EC	Timm et al., 2014
593	132	4.49	Brazil	No	PM	
596	132	4.52	Brazil	No	PM-FAO56	
411	124	3.31	Japan	Yes	Lysimeter	Shimono et al., 2013
185	113	4.29	IRRI-Flooded	Yes	EC, PM	Alberto et al., 2011
506	133	3.8	IRRI-AWD	Yes		
568	122	4.66	Italy-DF	No	PM	Facchi et al., 2013
578	122	5.56	Italy-DF	No		
591	120	5.76	Italy-AWD	No		
119-534	120	3.5-4.4	Japan	Yes	EC	Ikawa et al., 2017
95	147	4.05	Brazil	No	EC	Diaz et al., 2019
762	164	4.65		No		
577	164	4.13		No		
733	162	4.52		No		
716	154	4.65		No		
593	168	4.13		No		
551	133	4.14	Arkansas (this	No	EC	NF, 2015
501	143	4.20	study)	No		NF, 2016
528	138	4.55		No		NF, 2017
598	134	4.46		No		SF, 2015
604	143	4.22		No		SF, 2016
579	140	4.13		No		SF, 2017

that ET rates do not significantly differ between the different treatments. Other studies have indicated a similar range of mean growing season ET when compared to other conventional systems involving continuous flooding and AWD both domestically and internationally (Table 5). Based on this literature synthesis across methods, climate conditions, and production settings, estimated growing season ET ranged between 411 and 889 mm with daily ET rates ranging from 3.31 to 7.87 mm day<sup>-1</sup> (Table 5). When EC was used to measure ET directly, the range narrowed to 485 mm to 636 mm with measured daily ET between 3.50and 4.65 mm day<sup>-1</sup>. When only comparing studies reporting DAP, the median growing season ET was 653 mm with an equivalent ET rate of 4.87 mm day<sup>-1</sup>. Other methods, including the PM model, showed a much larger range of ET from 499 mm to 762 mm with estimated daily ET ranging between 4.05 and 4.65 mm day<sup>-1</sup>. Variation in estimated rates was likely linked to differences in climate conditions, method, and possibly production practices such as transplanting, which changes the scope or range of observation compared to direct seeding (Naklang et al., 1996; Tuong and Bhuiyan, 1999). With respect to metrics such as derived daily ET rate, the number of days after transplanting or direct seeding indicate different growth phases that can potentially differ in productivity (Dingkuhn et al., 1991).

#### 4.2. The effects of AWD on ET during the 2015 growing season

In our study, ET rates measured using eddy covariance showed no significant differences across the entire growing season and no significant differences during drying events when ET was expected to change due to the decline in WD. Regarding the drying events, neither field experienced major declines in volumetric water content (<20% VWC) that significantly influenced differences in ET between NF and SF. Studies conducted on field plots containing poorly drained clay soils have also reported similar results. Significant levels of drying relative to the study soils still yielded no significant differences in AWD and control yields (Carrijo et al., 2018; Norton et al., 2017). Because we observed no significant differences in yield quality or quantity between the treatments (Runkle et al., 2019), we assume with confidence that the plants were not significantly inhibited by water stress in grain production and associated transpiration. Thus, a large portion of ET remained unaffected by the AWD treatment. Additionally, the rice grown in both fields (XL745) was a hybrid variety associated with high nutrient efficiency and water-use efficiency to produce comparable yields in water-limited conditions (López-López et al., 2018). The combination of limited drying and the rice variety likely explained the lack of response in ET to drying events in both fields.

## 4.3. Modeling conductance using inverted PM

Across the daytime period, the estimated canopy conductance values from the inversion of the Penman–Monteith equation showed values ranging roughly between 3 and 33 mm s $^{-1}$ , which are similar to other studies estimating canopy conductance in rice across a number of studies (Table 6).

Canopy conductance estimates from various studies (Table 6) show comparable ranges to the current study, between 0 and 21 mm s $^{-1}$  during the growing season. Daily maximum conductance estimated from half hourly data throughout growing seasons ranged between 24 mm s $^{-1}$  (2016) and 28 mm s $^{-1}$  (2015) for NF and 20 mm s $^{-1}$  (2016) and 33 mm s $^{-1}$  (2017) for SF with peak values occurring between 1 PM and 5 PM for both fields when the canopy is most active. However, based on comparisons between the model and the initial estimates of conductance, the model was not able to accurately estimate conductance at any given time. A comparison of initial conductance estimates from the inverted PM–AET and known drivers of ET, such as net radiation and VPD, showed no apparent relationships during the daytime period throughout the growing season. While the parameterized model provided some definition to the relationships between environmental drivers and

**Table 6**Comparisons of estimated rice canopy conductance ranges under different production practices reported in studies.

Conductance range (mm $s^{-1}$ )	Irrigation Style	Location	Method	Author(s)
6–26	Controlled irrigation	Japan	Inverted PM & EC (daily mean over 5–day period in late season)	Miyata et al., 2000
0-20	Flooded	Japan (Saito)	Dual-Source	Maruyama
0-20	Flooded	Japan (Saga)	Heat transfer	and
0-30	Flooded	Japan (Aso)	model	Kuwagata,
		-	(based on	2010
			seasonal	
			observations)	
$16.55\pm8.99$	Flooded	Philippines	Inverted PM &	Alberto
		(2008, Dry	EC	et al., 2011
		Season)	(seasonal	
$8.85 \pm 4.51$	Aerobic	Philippines	mean)	
	(AWD)	(2008, Dry		
		Season)		
$12.47\pm6.39$	Flooded	Philippines		
		(2008, Wet		
		Season)		
$9.82 \pm 4.34$	Aerobic	Philippines		
	(AWD)	(2008, Wet		
$14.86 \pm 7.12$	Flooded	Season) Philippines		
$14.00 \pm 7.12$	riooded	(2009, Dry		
		Season)		
$8.91 \pm 3.35$	Aerobic	Philippines		
0.71 ± 0.00	(AWD)	(2009, Dry		
	()	Season)		
$18.24 \pm 7.98$	Flooded	Philippines		
		(2009, Wet		
		Season)		
$9.44 \pm 3.59$	Aerobic	Philippines		
	(AWD)	(2009, Wet		
		Season)		
0-16.86	DF	NF (2015)	Inverted PM &	This study
1.5–20.5	AWD	SF (2015)	EC	
0–15.56	AWD	NF (2016)	(seasonal	
0–14.09	AWD	SF (2016)	mean)	
0–13.53	DF	NF (2017)		
0–15.94	DF	SF (2017)		

conductance across each growing season, our results indicated that the rice canopy faced no apparent limitation based on VPD, available energy, or temperature with respect to conductance. However, the parameterized conductance was still able to generate more consistently accurate estimates of LE when compared to using a static monthly value for canopy conductance in the Penman–Monteith equation.

## 4.4. Improving PM-AET and PM-FAO56

In this study, the PM-AET approach estimated ET effectively across the growing season at the half-hourly time step. Because the model was constrained based on time of day due to the conductance modeling, ET estimates generated outside of the primary period are considered less reliable and less valuable when describing mechanistic relationships between drivers and associated ET. During the growing season, the canopy consistently experienced elevated levels of humidity (>80%) during the daytime period, reducing the overall atmospheric demand of water. We were also unable to detect significant responses in modeled stomatal conductance to changes in temperature and VPD, meaning the plants were not stressed despite the elevated temperatures and increased VPD. Available energy was the primary driver of ET throughout the growing season as evidenced through both direct observations and the use of the PM-AET, where measured available energy explained

significant amount of the variance in ET residuals between both fields. Regarding our hypotheses, we did not see any significant amount of variance between modeled and observed ET explained using soil moisture or water level across a variety of conditions in each growing season. As mentioned previously when addressing the effects of AWD, the canopy did not experience significant levels of drying below 40% VWC. Thus while we did not see a significant response, low soil moisture is known to impact canopy health (Carrijo et al., 2018). Additionally, the PM–AET method generated acceptable estimates of ET during the growing season regardless of irrigation regime.

Regarding the PM-FAO56 approach, it was clear that the current methodology produced comparable estimates of ET in 2015, but the model performance was inconsistent across the 2016 and 2017 growing seasons based on the comparison of cumulative ET amounts between the PM-FAO56 approach and the EC measurements. When observing the PM-FAO56 daily ET rates during the mid to late growing season, we saw the best performance in 2016, when both NF and SF were under AWD. Contrastingly, the model performance was poorest in years the precipitation was greater (2017) or the fields were kept under different management strategies (2015). Across the growing season, the estimated K<sub>c</sub> and recommended K<sub>c</sub> were more similar in the mid to late growing season. The dissimilarity between the estimated and recommended K<sub>c ini</sub> was likely due to the difference in production settings over which the coefficients were estimated. Water seeded rice production applies a substantially greater amount of water to the field during the early growing season compared to the drill seeding approach used in our experiments. Under flooded conditions at planting, the resulting ET would be higher compared to dry soil present in drill seeded rice, meaning the ratio of crop ET to reference ET would also be greater in the flooded field. This effect was reduced as the canopy developed in the later portion (DAP > 60) of the growing season, where variance was almost 50% less in the regression between EC derived values for  $K_{c, \mbox{\scriptsize mind}}$ and K<sub>c,end</sub> and the recommended FAO56 values.

However, the early growing season does not represent a period of time where producers are actively concerned with irrigation applications as the first flood has not been applied yet. Producer interest in using ET to schedule irrigation events would likely be tied to the mid and late growing season, when plant water availability is critical to maintaining profitable yields (Henry et al., 2013). Local climate likely played a role in differences in crop coefficient as the recommended crop coefficients were generated under climates that are less humid (Doorenbos and Pruitt, 1977; Doorenbos and Kassam, 1979). Considering our findings, we recommend that improvements to the method should include regional or site–specific crop coefficient development to better account for differences in production practices, such as water seeding vs. drill seeding. For practical applications, the PM-FAO56 method could still be a viable option for producers to estimate ET and schedule irrigation events.

The PM-AET model performed well as a method for gap filling LE fluxes at the half hourly time step. Based on our results with the PM-AET, capturing the amount of available energy as the difference between the net radiation and G is a critical component of estimating ET as demonstrated in our experiment. Because available energy represents such a large portion of ET in our production settings, less complex ET estimation methods such as the Priestley-Taylor (also a PM derivative) and the Hargreaves equation could prove to be valuable. Other studies based in rice across varying production systems have also identified available energy as the driving factor of ET in rice paddy systems with the ratio of LE to RN ranging from 71 to 74% during the typical growing period under flooded conditions (Hossen et al., 2012; Liu et al., 2019a,b; Timm et al., 2014). While establishing robust methodology and

application of tools is complex and multifaceted, development of methods for estimating ET at the canopy scale provides valuable information to better inform producers. Exploration and improved knowledge of modeling limitations and controls at the field scale can serve as a point of comparison for larger scale applications of ET modeling using remote sensing (Jiang and Ryu, 2016; Fisher et al., 2020).

#### 5. Conclusions

Based on this experiment's findings, the use of AWD as an irrigation treatment showed no significant effect on ET when compared to the conventional DF practice. The treatments showed no significant differences in yields, meaning that there was not significant water stress associated with drying events. If taken as a plant health indicator, ET was not affected and leads us to conclude that the plants did not experience drought stress and could still access sufficient water within the soil as VWC did not fall below 20% during drying events. We were able to use the PM-AET approach and conductance model to estimate halfhourly ET across the growing season. The model has potential to continue to provide mechanistic insight on driving environmental variables during different portions of the growing season with respect to ET. As seen in the comparison of field and recommended K<sub>c</sub>, the PM-FAO56 method did not yield strong results. We conclude that site-specific crop coefficient values are necessary to generate accurate crop coefficient values, especially during the early growing season. However, we also recognize that in practical application, ET during the mid-to-late growing season is more valuable for planning irrigation based on field ET estimates.

#### CRediT authorship contribution statement

Colby W. Reavis: Writing - original draft, Investigation, Data curation, Formal analysis, Visualization. Kosana Suvočarev: Writing - review & editing, Investigation, Methodology. Michele L. Reba: Writing - review & editing, Investigation, Resources, Methodology. Benjamin R.K. Runkle: Writing - review & editing, Investigation, Data curation, Conceptualization, Supervision.

## **Declaration of Competing Interest**

The authors declare that they have no known competing financial interests or personal relationships that could have appeared to influence the work reported in this paper.

#### Acknowledgements

We thank the Isbell family's Zero Grade Farms for hosting and helping manage our experiment and Allison Sites, Zach Johnson, Bryant Fong, Yin–Lin Chiu and W. Jonathon Delp, for field and data analysis support. We thank Merle Anders for his contributions. We thank Cove Sturtevant of NEON for sharing Matlab code used to gap–fill flux data with artificial neural networks.

This work has been funded through the U.S. Geological Survey under Cooperative Agreements G11AP20066 and G16AP00040 as administered by the Arkansas Water Resources Center at the University of Arkansas; the USDA–NRCS under Cooperative Agreement 68–7103–17–119, and the NSF under CBET Award 1752083. The views and conclusions contained in this document are those of the authors and do not represent the opinions or policies of the USGS or the Department of Agriculture; use of trade names and commercial products does not constitute endorsement.

#### Appendix A

Aerodynamic resistance  $(r_a)$ 

Aerodynamic resistance was calculated using the following equation presented as a part of FAO 56 document with regards to the Penman–Monteith equation:

$$r_a = \frac{ln \left(\frac{z_m - d}{z_{om}}\right) * ln \left(\frac{z_h - d}{z_{oh}}\right)}{k^2 * u_z}$$

$$d = \frac{2}{3} * h$$

$$z_{om} = 0.123*h$$

$$z_{oh} = 0.1 * z_{om}$$

where  $r_a$  is aerodynamic resistance, s m<sup>-1</sup>,  $z_m$  is height of wind measurements in meters (2.2 m),  $z_h$  is height of humidity measurements in meters (2.2 m), d is zero plane displacement height in meters,  $z_{om}$  is roughness length governing momentum transfer in meters,  $z_{oh}$  is roughness length governing transfer of heat and vapor in meters, k is von Karman's constant, 0.41,  $u_z$  is wind speed at height z, m s<sup>-1</sup>.

#### Crop coefficient adjustments

For the initial crop coefficient,  $K_{c,ini}$ , FAO56 recommends a value of 1.05 for rice. The document also provides adjustments based on wind speed and humidity. Our site was classified as very humid with moderate to strong winds, meaning the initial value could be between 1.05 and 1.10 based on Table 14 in Chapter 6 of FAO 56. For this study, we used 1.05 as  $K_{c,ini}$ .

For the mid–season crop coefficient and end crop coefficient,  $K_{c,mid}$  and  $K_{c,end}$ , similar adjustments were made based on relative humidity, wind speed, and canopy height using the equation:

$$K_{c,mid(end)} = K_{c,mid(end),rec} + \left[0.4*(u_2 - 2) - 0.004(RH_{min} - 45)\right] \left(\frac{h}{3}\right)^{0.3}$$

where  $K_{c,mid (end),rec}$  is the recommended value for the middle or end of the growing season taken from Table 12 of FAO56 (1.2 and 1.0, respectively),  $u_2$  is the daily wind speed at 2 m during the mid–season or end growth stage,  $RH_{min}$  is the daily minimum during the mid–season or end growth stage, respectively,  $w_0$ , and  $w_0$  is mean plant height during the mid–season or end growth stage, respectively,  $w_0$ .

#### References

- Alberto, M.C.R., Quilty, J.R., Buresh, R.J., Wassmann, R., Haidar, S., Correa, T.Q., Sandro, J.M., 2014. Actual evapotranspiration and dual crop coefficients for dry-seeded rice and hybrid maize grown with overhead sprinkler irrigation. Agric. Water Manag. 136, 1–12. https://doi.org/10.1016/j.agwat.2014.01.005.
- Alberto, M.C.R., Wassmann, R., Hirano, T., Miyata, A., Hatano, R., Kumar, A., Padre, A., Amante, M., 2011. Comparisons of energy balance and evapotranspiration between flooded and aerobic rice fields in the Philippines. Agric. Water Manag. 98 (9), 1417–1430. https://doi.org/10.1016/j.agwat.2011.04.011.
- Allen, R.G., Pereira, L.S., Raes, D., Smith, M., 1998. Crop evapotranspiration Guidelines for computing crop water requirements – FAO Irrigation and drainage paper 56. FAO, Rome 300, D05109.
- Carrijo, D.R., Akbar, N., Reis, A.F.B., Li, C., Gaudin, A.C.M., Parikh, S.J., Green, P.G., Linquist, B.A., 2018. Impacts of variable soil drying in alternate wetting and drying rice systems on yields, grain arsenic concentration and soil moisture dynamics. Field Crops Res. 222. 101–110. https://doi.org/10.1016/i.fcr.2018.02.026.
- Carrijo, D.R., Lundy, M.E., Linquist, B.A., 2017. Rice yields and water use under alternate wetting and drying irrigation: a meta–analysis. Field Crops Res. 203, 173–180. https://doi.org/10.1016/j.fcr.2016.12.002.
- Collatz, G.J., Ball, J.T., Grivet, C., Berry, J.A., 1991. Physiological and environmental regulation of stomatal conductance, photosynthesis and transpiration: a model that includes a laminar boundary layer. Agric. For. Meteorol. 54 (2-4), 107–136. https:// doi.org/10.1016/0168-1923(91)90002-8.
- Diaz, M.B., Roberti, D.R., Carneiro, J.V., Souza, V. de A., de Moraes, O.L.L., 2019. Dynamics of the superficial fluxes over a flooded rice paddy in southern Brazil. Agric. For. Meteorol. 276–277, 107650 https://doi.org/10.1016/j. agr/cremet 2019 107650
- Dingkuhn, M., Schnier, H.F., De Datta, S.K., Dorffling, K., Javellana, C., 1991.
  Relationships between ripening-phase productivity and crop duration, canopy photosynthesis and senescence in transplanted and direct-seeded lowland rice. Field Crops Res. 26 (3-4), 327–345. https://doi.org/10.1016/0378-4290(91)90009-K.
  Doorenbos, J., Kassam, A., 1979. Yield response to water, Irrig, Drain, 257, 33.
- Doorenbos, J., Pruitt, W.O., 1977. Crop water requirements. FAO irrigation and drainage paper 24. Land and Water Development Division, FAO, Rome 144.

- Ershadi, A., McCabe, M.F., Evans, J.P., Wood, E.F., 2015. Impact of model structure and parameterization on Penman-Monteith type evaporation models. J. Hydrol. 525, 521–535. https://doi.org/10.1016/j.jhydrol.2015.04.008.
- Facchi, A., Gharsallah, O., Chiaradia, E.A., Bischetti, G.B., Gandolfi, C., 2013. Monitoring and modelling evapotranspiration in flooded and aerobic rice fields. Procedia Environ. Sci. 19, 794–803.
- Fisher, J.B., Lee, B., Purdy, A.J., Halverson, G.H., Dohlen, M.B., Cawse-Nicholson, K., Wang, A., Anderson, R.G., Aragon, B., Arain, M.A., Baldocchi, D.D., Baker, J.M., Barral, H., Bernacchi, C.J., Bernhofer, C., Biraud, S.C., Bohrer, G., Brunsell, N., Cappelaere, B., Castro-Contreras, S., Chun, J., Conrad, B.J., Cremonese, E., Demarty, J., Desai, A.R., Ligne, A.D., Foltýnová, L., Goulden, M.L., Griffis, T.J., Grünwald, T., Johnson, M.S., Kang, M., Kelbe, D., Kowalska, N., Lim, J.-H., Maïnassara, I., McCabe, M.F., Missik, J.E.C., Mohanty, B.P., Moore, C.E., Morillas, L., Morrison, R., Munger, J.W., Posse, G., Richardson, A.D., Russell, E.S., Ryu, Y., Sanchez-Azofeifa, A., Schmidt, M., Schwartz, E., Sharp, I., Sigut, L., Tang, Y., Hulley, G., Anderson, M., Hain, C., French, A., Wood, E., Hook, S., 2020. ECOSTRESS: NASA's Next Generation Mission to Measure Evapotranspiration From the International Space Station. Water Resour. Res. 56 https://doi.org/10.1029/2019WR026058 e2019WR026058.
- Fuchs, M., Tanner, C.B., 1968. Calibration and field test of soil heat flux plates. Soil Sci. Soc. Am. J. 32 (3), 326–328. https://doi.org/10.2136/sssai1968.03615995003200030021x.
- Gardiol, J.M., Serio, L.A., Della Maggiora, A.I., 2003. Modelling evapotranspiration of corn (Zea mays) under different plant densities. J. Hydrol. 271 (1-4), 188–196. https://doi.org/10.1016/S0022-1694(02)00347-5.
- Gharsallah, O., Facchi, A., Gandolfi, C., 2013. Comparison of six evapotranspiration models for a surface irrigated maize agro-ecosystem in Northern Italy. Agric. Water Manag. 130, 119–130.
- Graham-Acquaah, S., Siebenmorgen, T.J., Reba, M.L., Massey, J.H., Mauromoustakos, A., Adviento-Borbe, A., January, R., Burgos, R., Baltz-Gray, J., 2019. Impact of alternative irrigation practices on rice quality. Cereal Chem. 96 (5), 815–823. https://doi.org/10.1002/cche.v96.510.1002/cche.10182.
- Hargreaves, G.H., Allen, R.G., 2003. History and evaluation of hargreaves evapotranspiration equation. J. Irrig. Drain. Eng. 129 (1), 53–63. https://doi.org/ 10.1061/(ASCE)0733-9437(2003)129-1(53)
- Henry, C.G., Daniels, M., Hamilton, M., Hardke, J., 2013. Water Management. Arkansas Rice Production Handbook MP, 192. pp. 103–128.

Journal of Hydrology 596 (2021) 126080

- Henry, C.G., Hirsh, S.L., Anders, M.M., Vories, E.D., Reba, M.L., Watkins, K.B., Hardke, J. T., 2016. Annual irrigation water use for arkansas rice production. J. Irrig. Drain. Eng. 142 (11), 05016006. https://doi.org/10.1061/(ASCE)IR.1943-4774.0001068.
- Horst, T.W., Semmer, S.R., Maclean, G., 2015. Correction of a non-orthogonal, three-component sonic anemometer for flow distortion by transducer shadowing. Boundary-Layer Meteorol. 155 (3), 371–395. https://doi.org/10.1007/s10546-015-0010-3.
- Hossen, M.S., Mano, M., Miyata, A., Baten, M.A., Hiyama, T., 2012. Surface energy partitioning and evapotranspiration over a double–cropping paddy field in Bangladesh. Hydrol. Process. 26 (9), 1311–1320. https://doi.org/10.1002/hyp. v26.910.1002/hyp.8232.
- Ikawa, H., Chen, C.P., Sikma, M., Yoshimoto, M., Sakai, H., Tokida, T., Usui, Y., Nakamura, H., Ono, K., Maruyama, A., Watanabe, T., Kuwagata, T., Hasegawa, T., 2018. Increasing canopy photosynthesis in rice can be achieved without a large increase in water use—a model based on free-air CO2 enrichment. Global Change Biol. 24, 1321–1341. https://doi.org/10.1111/gcb.13981.
- Ikawa, H., Ono, K., Mano, M., Kobayashi, K., Takimoto, T., Kuwagata, T., Miyata, A., 2017. Evapotranspiration in a rice paddy field over 13 crop years. J. Agric. Meteorol. 73 (3), 109–118. https://doi.org/10.2480/agrmet.D-16-00011.
- Jarvis, P.G., Monteith, J.L., Weatherley, P.E., 1976. The interpretation of the variations in leaf water potential and stomatal conductance found in canopies in the field. Philos. Trans. R. Soc. London B, Biol. Sci. 273, 593–610. https://doi.org/10.1098/ rstb.1976.0035.
- Jiang, C., Ryu, Y., 2016. Multi-scale evaluation of global gross primary productivity and evapotranspiration products derived from Breathing Earth System Simulator (BESS). Remote Sens. Environ. 186, 528–547.
- Keisling, T., Wells, B.R., Davis, G.L., 1984. Rice Management Decision Aids Based Upon Thermal Time Base 50°. Cooperative Extension Service, University of Arkansas, USDA, and county governments cooperating.
- Kima, A.S., Chung, W.G., Wang, Y.-M., Traoré, S., 2015. Evaluating water depths for high water productivity in irrigated lowland rice field by employing alternate wetting and drying technique under tropical climate conditions, Southern Taiwan. Paddy Water Environ. 13 (4), 379–389. https://doi.org/10.1007/s10333-014-0458-7.
- Knox, S.H., Matthes, J.H., Sturtevant, C., Oikawa, P.Y., Verfaillie, J., Baldocchi, D., 2016. Biophysical controls on interannual variability in ecosystem–scale CO2 and CH4 exchange in a California rice paddy. J. Geophys. Res.: Biogeosci. 121 (3), 978–1001. https://doi.org/10.1002/2015JG003247.
- Knox, S.H., Sturtevant, C., Matthes, J.H., Koteen, L., Verfaillie, J., Baldocchi, D., 2015. Agricultural peatland restoration: effects of land-use change on greenhouse gas (CO2 and CH4) fluxes in the Sacramento-San Joaquin Delta. Global Change Biolo. 21 (2), 750–765. https://doi.org/10.1111/gcb.12745.
- Kotani, A., Hiyama, T., Ohta, T., Hanamura, M., Kambatuku, J.R., Awala, S.K., Iijima, M., 2017. Impact of rice cultivation on evapotranspiration in small seasonal wetlands of north-central Namibia. Hydrol. Res. Lett. 11, 134–140. https://doi.org/10.3178/ hrl 11 134
- Kresse, T.M., Hays, P.D., Merriman, K.R., Gillip, J.A., Fugitt, D.T., Spellman, J.L., Nottmeier, A.M., Westerman, D.A., Blackstock, J.M., Battreal, J.L., 2014. Aquifers of Arkansas: protection, management, and hydrologic and geochemical characteristics of groundwater resources in Arkansas (USGS Numbered Series No. 2014–5149). Aquifers of Arkansas: protection, management, and hydrologic and geochemical characteristics of groundwater resources in Arkansas, Scientific Investigations Report. U.S. Geological Survey, Reston, VA. https://doi.org/10.3133/sir20145149.
- Lafleur, P.M., Rouse, W.R., 1990. Application of an energy combination model for evaporation from sparse canopies. Agric. For. Meteorol. 49 (2), 135–153.
- Lampayan, R.M., Rejesus, R.M., Singleton, G.R., Bouman, B.A.M., 2015. Adoption and economics of alternate wetting and drying water management for irrigated lowland rice. Field Crops Res. 170, 95–108. https://doi.org/10.1016/j.fcr.2014.10.013.
  Lecina, S., Martínez-Cob, A., Pérez, P.J., Villalobos, F.J., Baselga, J.J., 2003. Fixed versus
- Lecina, S., Martínez-Cob, A., Pérez, P.J., Villalobos, F.J., Baselga, J.J., 2003. Fixed versus variable bulk canopy resistance for reference evapotranspiration estimation using the Penman-Monteith equation under semiarid conditions. Agric. Water Manag. 60 (3), 181–198. https://doi.org/10.1016/S0378-3774(02)00174-9.
  Leuning, R., Kelliher, F.M., Pury, D.G.G., Schulze, E.-D., 1995. Leaf nitrogen,
- Leuning, R., Kelliher, F.M., Pury, D.G.G., Schulze, E.-D., 1995. Leaf nitrogen, photosynthesis, conductance and transpiration: scaling from leaves to canopies. Plant, Cell Environ. 18 (10), 1183–1200. https://doi.org/10.1111/j.1365-3040.1995.tb00628.x
- Li, X., Kang, S., Li, F., Jiang, X., Tong, L., Ding, R., Li, S., Du, T., 2016. Applying segmented Jarvis canopy resistance into Penman-Monteith model improves the accuracy of estimated evapotranspiration in maize for seed production with film–mulching in arid area. Agric. Water Manag. 178, 314–324. https://doi.org/10.1016/j.agwat.2016.09.016.
- Li, Y.H., Cui, Y.L., 1996. Real-time forecasting of irrigation water requirements of paddy fields. Agric. Water Manag. 31 (3), 185–193. https://doi.org/10.1016/0378-3774 (96)01252-8.
- Linquist, B.A., Anders, M.M., Adviento-Borbe, M.A.A., Chaney, R.L., Nalley, L.L., da Rosa, E.F.F., van Kessel, C., 2015a. Reducing greenhouse gas emissions, water use, and grain arsenic levels in rice systems. Global Change Biol. 21 (1), 407–417. https://doi.org/10.1111/gcb.12701.
- Linquist, B., Snyder, R., Anderson, F., Espino, L., Inglese, G., Marras, S., Moratiel, R., Mutters, R., Nicolosi, P., Rejmanek, H., Russo, A., Shapland, T., Song, Z., Swelam, A., Tindula, G., Hill, J., 2015b. Water balances and evapotranspiration in water–and dry–seeded rice systems. Irrig. Sci. 33 (5), 375–385.
- Linquist, B.A., Marcos, M., Adviento-Borbe, M.A., Anders, M., Harrell, D., Linscombe, S., Reba, M.L., Runkle, B.R.K., Tarpley, L., Thomson, A., 2018. Greenhouse gas emissions and management practices that affect emissions in US rice systems.
  J. Environ. Qual. 47 (3), 395–409. https://doi.org/10.2134/jeq2017.11.0445.

- Liu, B., Cui, Y., Luo, Y., Shi, Y., Liu, M., Liu, F., 2019a. Energy partitioning and evapotranspiration over a rotated paddy field in Southern China. Agric. For. Meteorol. 276-277, 107626. https://doi.org/10.1016/j.agrformet.2019.107626.
- Liu, X., Xu, J., Yang, S., Lv, Y., 2019b. Surface energy partitioning and evaporative fraction in a water-saving irrigated rice field. Atmosphere 10, 51. https://doi.org/ 10.3390/atmos10020051.
- Liu, X., Xu, J., Wang, W., Lv, Y., Li, Y., 2020. Modeling rice evapotranspiration under water-saving irrigation condition: Improved canopy-resistance-based. J. Hydrol. 590, 125435. https://doi.org/10.1016/j.jhydrol.2020.125435.
- López-López, R., Jiménez-Chong, José.A., Hernández-Aragón, L., Inzunza Ibarra, M.A., 2018. Water productivity of rice genotypes with irrigation and drainage. Irrig. Drain. 67 (4), 508–515. https://doi.org/10.1002/ird.v67.410.1002/ird.2250.
- Massey, J.H., Smith, M.C., Vieira, D.A.N., Adviento-Borbe, M.A., Reba, M.L., Vories, E.D., 2018. Expected irrigation reductions using multiple-inlet rice irrigation under rainfall conditions of the Lower Mississippi River Valley. J. Irrig. Drain. Eng. 144 (7), 04018016. https://doi.org/10.1061/(ASCE)IR.1943-4774.0001303.
- Maruyama, A., Kuwagata, T., 2010. Coupling land surface and crop growth models to estimate the effects of changes in the growing season on energy balance and water use of rice paddies. Agricul. Forest Meteorol. 150, 919–930.
- Massey, J.H., Mark Stiles, C., Epting, J.W., Shane Powers, R., Kelly, D.B., Bowling, T.H., Leighton Janes, C., Pennington, D.A., 2017. Long-term measurements of agronomic crop irrigation made in the Mississippi delta portion of the lower Mississippi River Valley. Irrig Sci 35 (4), 297–313. https://doi.org/10.1007/s00271-017-0543-y.
- Massey, J.H., Walker, T.W., Anders, M.M., Smith, M.C., Avila, L.A., 2014. Farmer adaptation of intermittent flooding using multiple-inlet rice irrigation in Mississippi. Agricul. Water Manage. 146, 297–304. https://doi.org/10.1016/j. agwat.2014.08.023.
- Miyata, A., Leuning, R., Denmead, O.T., Kim, J., Harazono, Y., 2000. Carbon dioxide and methane fluxes from an intermittently flooded paddy field. Agricul. Forest Meteorol. 102, 287–303. https://doi.org/10.1016/S0168-1923(00)00092-7.
- Moldenhauer, K., Conce, P., Hardke, J., 2013. Rice Growth and Development. Arkansas Rice Production Handbook MP 192, 9–20.
- Monteith, J.L., 1965. Evaporation and environment. Symposia of the Society for Experimental Biology 19, 205–234.
- Moran, M.S., Maas Jr, S.J., P.J.P., 1995. Combining remote sensing and modeling for estimating surface evaporation and biomass production. Remote Sens. Rev. 12, 335–353. https://doi.org/10.1080/02757259509532290.
- Mote, K., Rao, V.P., Kumar, K.A., Ramulu, V., 2018. Estimation of crop evapotranspiration and crop coefficients of rice (Oryza sativa L.) under low land condition. J. Agrometeorol. Anand 20, 117–121.
- Myneni, R., Knyazikhin, Y., Park, T., 2015. MOD15A2H MODIS/Terra Leaf Area Index/FPAR 8-Day L4 Global 500m SIN Grid V006. NASA EOSDIS Land Processes DAAC. Accessed 2020-03-27 from <a href="https://doi.org/10.5067/MODIS/MODI5A2H.006">https://doi.org/10.5067/MODIS/MODI5A2H.006</a>.
- Naklang, K., Shu, F., Nathabut, K., 1996. Growth of rice cultivars by direct seeding and transplanting under upland and lowland conditions. Field Crops Res. 48 (2-3), 115–123. https://doi.org/10.1016/S0378-4290(96)01029-5.
- Nalley, L., Linquist, B., Kovacs, K., Anders, M., 2015. The economic viability of alternative wetting and drying irrigation in Arkansas rice production. Agron. J. 107 (2), 579–587. https://doi.org/10.2134/agronj14.0468.
- Norman, J.M., Kustas, W.P., Humes, K.S., 1995. Source approach for estimating soil and vegetation energy fluxes in observations of directional radiometric surface temperature. Agric. For. Meteorol., Therm. Remote Sens. Energy Water Balance over Veg. 77 (3-4), 263–293. https://doi.org/10.1016/0168-1923(95)02265-Y.
- Norton, G.J., Shafaei, M., Travis, A.J., Deacon, C.M., Danku, J., Pond, D., Cochrane, N., Lockhart, K., Salt, D., Zhang, H., Dodd, I.C., Hossain, M., Islam, M.R., Price, A.H., 2017. Impact of alternate wetting and drying on rice physiology, grain production, and grain quality. Field Crops Res. 205, 1–13. https://doi.org/10.1016/j.fcr.2017.01.016.
- ORNL DAAC 2018. MODIS and VIIRS Land Products Global Subsetting and Visualization Tool. ORNL DAAC, Oak Ridge, Tennessee, USA. Accessed Jan 1, 2019. Subset obtained for MCD15A3H product at 34.586070, -91.749620, time period: Jan 1, 2015 to Dec 31, 2017, and subset size: 1 x 1 km. https://doi.org/10.3334/ORNL DAAC/1379.
- Pan, J., Liu, Y., Zhong, X., Lampayan, R.M., Singleton, G.R., Huang, N., Liang, K., Peng, B., Tian, K., 2017. Grain yield, water productivity and nitrogen use efficiency of rice under different water management and fertilizer-N inputs in South China. Agric. Water Manag. 184, 191–200. https://doi.org/10.1016/j.agwat.2017.01.013.
- Penman, H.L., 1948. Natural evaporation from open water, bare soil and grass.

  Proceedings of the Royal Society of London. Series A. Mathematical and Physical Sciences 193, 120–145.
- Pereira, L.S., Allen, R.G., Smith, M., Raes, D., 2015. Crop evapotranspiration estimation with FAO56: Past and future. Agric. Water Manag.: Prior. Challenges 147, 4–20. https://doi.org/10.1016/j.agwat.2014.07.031.
- Reba, M.L., Daniels, M., Chen, Y., Sharpley, A., Bouldin, J., Teague, T.G., Daniel, P., Henry, C.G., 2013. A statewide network for monitoring agricultural water quality and water quantity in Arkansas. J. Soil Water Conserv. 68 (2), 45A–49A. https://doi. org/10.2489/jswc.68.2.45A.
- Reba, M.L., Massey, J.H., Adviento-Borbe, M.A., Leslie, D., Yaeger, M.A., Anders, M., Farris, J., 2017. Aquifer depletion in the lower Mississippi river basin: challenges and solutions. J. Contemp. Water Res. Educ. 162 (1), 128–139. https://doi.org/10.1111/j.1936-704X.2017.03264.x.
- Roel, A., Heilman, J.L., McCauley, G.N., 1999. Water use and plant response in two rice irrigation methods. Agric. Water Manag. 39 (1), 35–46. https://doi.org/10.1016/ \$0378.3774(98)00087.0
- Runkle, B.R.K., Rigby, J.R., Reba, M.L., Anapalli, S.S., Bhattacharjee, J., Krauss, K.W., Liang, L., Locke, M.A., Novick, K.A., Sui, R., Suvočarev, K., White, P.M., 2017.

- Delta–Flux: An Eddy Covariance network for a climate-smart lower Mississippi Basin. Agric. Environ. Lett. 2 (1) https://doi.org/10.2134/ael2017.01.0003.
- Runkle, B.R.K., Suvočarev, K., Reba, M.L., Reavis, C.W., Smith, S.F., Chiu, Y.-L., Fong, B., 2019. Methane emission reductions from the alternate wetting and drying of rice fields detected Using the Eddy Covariance Method. Environ. Sci. Technol. 53 (2), 671–681. https://doi.org/10.1021/acs.est.8b05535.s001.
- Shimono, H., Nakamura, H., Hasegawa, T., Okada, M., 2013. Lower responsiveness of canopy evapotranspiration rate than of leaf stomatal conductance to open-air CO2 elevation in rice. Global Change Biol. 19, 2444–2453. https://doi.org/10.1111/ gcb.12214.
- Shuttleworth, W.J., Wallace, J.S., 1985. Evaporation from sparse crops-an energy combination theory. Q. J. R. Meteorol. Soc. 111 (469), 839–855.
- Smith, M., 1992. CROPWAT: a computer program for irrigation planning and management. Food Agric. Org.
- Soil Survey Staff, Natural Resources Conservation Service, United States Department of Agriculture, 2018. Web Soil Survey. Available at: <a href="https://websoilsurvey.sc.egov.usda.gov">https://websoilsurvey.sc.egov.usda.gov</a> (accessed 12.3.18).
- Sudhir-Yadav, Humphreys, E., Li, T., Gill, G., Kukal, S.S., 2012. Evaluation of tradeoffs in land and water productivity of dry seeded rice as affected by irrigation schedule. Field Crops Res. 128, 180–190. https://doi.org/10.1016/j.fcr.2012.01.005.
- Suvočarev, K., Castellví, F., Reba, M.L., Runkle, B.R.K., 2019. Surface renewal measurements of H, λE and CO2 fluxes over two different agricultural systems. Agric. For. Meteorol. 279, 107763. https://doi.org/10.1016/j.agrformet.2019.107763.
- Timm, A.U., Roberti, D.R., Streck, N.A., Gonçalvesde, L.G.G., Acevedo, O.C., Moraes, O. L.L., Moreira, V.S., Degrazia, G.A., Ferlan, M., Toll, D.L., 2014. Energy Partitioning and Evapotranspiration over a Rice Paddy in Southern Brazil. J. Hydrometeorol. 15, 1975–1988. https://doi.org/10.1175/JHM-D-13-0156.1.
- Tuong, T.P., Bhuiyan, S.I., 1999. Increasing water-use efficiency in rice production: farm-level perspectives. Agric. Water Manag. 40 (1), 117–122. https://doi.org/10.1016/S0378-3774(98)00091-2.

- Wang, H., Zhang, Y., Zhang, Y., McDaniel, M.D., Sun, L., Su, W., Fan, X., Liu, S., Xiao, X., 2020. Water-saving irrigation is a 'win-win' management strategy in rice paddies With both reduced greenhouse gas emissions and enhanced water use efficiency. Agric. Water Manage. 228, 105889. https://doi.org/10.1016/j.agwat.2019.105889.
- Wang, Y., Zhou, L., Jia, Q., Yu, W., 2017. Water use efficiency of a rice paddy field in Liaohe Delta, Northeast China. Agric. Water Manag. 187, 222–231. https://doi.org/ 10.1016/j.agwat.2017.03.029.
- Wei, Z., Yoshimura, K., Okazaki, A., Kim, W., Liu, Z., Yokoi, M., 2015. Partitioning of evapotranspiration using high-frequency water vapor isotopic measurement over a rice paddy field. Water Resour. Res. 51 (5), 3716–3729. https://doi.org/10.1002/ 2014WR016737.
- Wei, Z., Yoshimura, K., Wang, L., Miralles, D.G., Jasechko, S., Lee, X., 2017. Revisiting the contribution of transpiration to global terrestrial evapotranspiration. Geophys. Rese. Lett. 44 (6), 2792–2801. https://doi.org/10.1002/2016GL072235.
- Xu, J., Liu, X., Yang, S., Qi, Z., Wang, Y., 2017. Modeling rice evapotranspiration under water–saving irrigation by calibrating canopy resistance model parameters in the Penman-Monteith equation. Agric. Water Manag. 182, 55–66. https://doi.org/ 10.1016/j.agwat.2016.12.010.
- Xu, J., Wu, B., Yan, N., Tan, S., 2018. Regional daily ET estimates based on the gap-filling method of surface conductance. Remote Sens. 10, 554. https://doi.org/10.3390/ re10040554
- Yan, H., Zhang, C., Hiroki, O., 2018. Parameterization of canopy resistance for modeling the energy partitioning of a paddy rice field. Paddy Water Environ. 16 (1), 109–123. https://doi.org/10.1007/s10333-017-0620-0.
- Yang, S., Logan, J., Coffey, D.L., 1995. Mathematical formulae for calculating the base temperature for growing degree days. Agric. For. Meteorol. 74 (1-2), 61–74. https://doi.org/10.1016/0168-1923(94)02185-M.
- Zhang, B., Kang, S., Li, F., Zhang, L., 2008. Comparison of three evapotranspiration models to Bowen ratio–energy balance method for a vineyard in an arid desert region of northwest China. Agric. For. Meteorol. 148 (10), 1629–1640. https://doi. org/10.1016/j.agrformet.2008.05.016.